Scattering from very rough layers under the geometric optics approximation: further investigation

Nicolas Pinel* and Christophe Bourlier

IREENA (Institut de Recherche en Electrotechnique et Electronique de Nantes Atlantique), Radar Team, Polytech'Nantes, Rue Christian Pauc, La Chantrerie, BP 50609, 44306 Nantes Cedex 3, France
**Corresponding author: nicolas.pinel@univ-nantes.fr*

Received February 4, 2008; accepted March 14, 2008;
posted March 24, 2008 (Doc. ID 92475); published May 14, 2008

Scattering from very rough homogeneous layers is studied in the high-frequency limit (under the geometric optics approximation) by taking the shadowing effect into account. To do so, the iterated Kirchhoff approximation, recently developed by Pinel *et al.* [Waves Random Complex Media **17**, 283 (2007)] and reduced to the geometric optics approximation, is used and investigated in more detail. The contributions from the higher orders of scattering inside the rough layer are calculated under the iterated Kirchhoff approximation. The method can be applied to rough layers of either very rough or perfectly flat lower interfaces, separating either lossless or lossy media. The results are compared with the PILE (propagation-inside-layer expansion) method, recently developed by Déchamps *et al.* [J. Opt. Soc. Am. A **23**, 359 (2006)], and accelerated by the forward-backward method with spectral acceleration. They highlight that there is very good agreement between the developed method and the reference numerical method for all scattering orders and that the method can be applied to root-mean-square (RMS) heights at least down to 0.25λ.

OCIS codes: 290.5880, 000.5490, 280.0280.

1. INTRODUCTION

First, let us define the following acronyms:

- KA: Kirchhoff approximation
- KA1: First-order Kirchhoff approximation
- IKA: Iterated Kirchhoff approximation
- GOA: Geometric optics approximation
- PILE: Propagation-inside-layer expansion method
- FB-SA: Forward-backward method with spectral acceleration

Bistatic electromagnetic scattering from dielectric homogeneous rough layers has many applications. In the remote sensing domain, it can be used to detect ocean ice, sand cover of arid regions, or oil slicks on the ocean. In the optics domain, it can be useful, for instance, in optical studies of thin films and coated surfaces and in treatment of antireflection coatings. The use of *fast* asymptotic models can then be of practical interest to predict the scattered signal of such systems.

The study focuses here on the case of very rough homogeneous layers, i.e., on layers for which the considered rough surfaces are very rough compared to the wavelength (we will refine this point later). As stated in the Introduction of [1], to our knowledge, no preceding asymptotic method allowed one to present numerical results for very rough homogeneous layers. This recently developed method [1], which we can call the iterated Kirchhoff approximation (IKA), can deal with either perfectly flat or very rough lower interfaces, the upper interface being very rough.

The objective of the IKA is to obtain a simple mathematical expression of the bistatic scattering coefficient in the high-frequency limit (taking the shadowing effect into account) in order to get a *fast method* for solving the problem of very rough homogeneous layers: Then in this model the Kirchhoff approximation (KA), which is used at each scattering point inside the dielectric rough layer, is reduced to the geometric optics approximation (GOA).

The starting point of the method is the KA [2–6], applicable to surfaces with large radii of curvature compared to the incident electromagnetic wavelength. The model uses the widely used KA in reflection, but also the KA in transmission [4–6], which allows one to obtain the fields reflected onto and transmitted through a rough interface. This paper presents the reflection and transmission scattering coefficients associated with a stack of two rough interfaces and a rough interface overlying a perfectly flat interface, in which the KA is iterated for each successive scattering in reflection or transmission on the rough interface(s). The paper focuses on one-dimensional stationary random rough surfaces and takes the shadowing effect into account [7–9].

In Section 2 of the paper, the expressions of the first- and second-order scattering coefficients of the method are recalled in the high-frequency limit (using the GOA). Then the higher-order scattering coefficients of the method are derived. A detailed analysis of the validity domain of the method is to follow. Last, in Section 3 numerical results are presented and compared with a benchmark numerical method based on the method of moments to validate the asymptotic model and to check its validity domain. The chosen reference method is the PILE (propagation-inside-layer expansion) method [10,11] accelerated by the forward-backward method [12] with spectral acceleration (FB-SA) [13–16].

2. ITERATED KIRCHHOFF APPROXIMATION

The studied system (see Fig. 1) is composed of a stack of two rough interfaces (Σ_A for the upper interface; Σ_B for the lower interface) separating homogeneous media Ω_α ($\alpha=\{1,2,3\}$). The three media Ω_α, with relative permittivity $\epsilon_{r\alpha}$, are assumed to be nonmagnetic (relative permeability $\mu_{r\alpha}=1$).

A. First Two Contributions in Reflection and First Contribution in Transmission

The calculation of the first-order reflection scattering coefficient $\sigma_{r,1}$, obtained from the statistical correlation of $E_{r,1}$ and corresponding to the scattering in reflection from the upper interface, is relatively simple. It is defined by [1]

$$\sigma_{r,1}=\frac{1}{\cos\theta_i}|r_{12}(\chi_{ri}^0)f(\boldsymbol{k}_i,\boldsymbol{k}_r;\boldsymbol{n}_{ri}^0)|^2\frac{p_s(\gamma_{ri}^0)}{|\hat{q}_r-\hat{q}_i|}S_{11}(\boldsymbol{k}_i,\boldsymbol{k}_r|\gamma_{ri}^0), \quad (1)$$

with $\gamma_{ri}^0=-(k_r-k_i)/(q_r-q_i)$; $S_{11}(\boldsymbol{k}_i,\boldsymbol{k}_r|\gamma_{ri}^0)$ is the average bistatic reflection shadowing function expressed by Bourlier *et al.* [7]; r_{ij} represents the Fresnel reflection coefficient from the medium Ω_i onto the medium Ω_j; $f(\boldsymbol{k}_i,\boldsymbol{k}_r;\boldsymbol{n}_{ri}^0)$ is a projection term onto the rough surface with $\boldsymbol{n}_{ri}^0$ the normal that reflects the incident wave of direction $\boldsymbol{k}_i$ specularly in the direction $\boldsymbol{k}_r$; and p_s is the surface slope probability density function (PDF). One can observe that this scattering coefficient is independent of both the frequency and the surface height statistics and can be applied for any given slope statistics.

In contrast, the calculation of the second-order reflection scattering coefficient $\sigma_{r,2}$ is much more complicated. This nontrivial calculation was not presented before; therefore it is reported here in Appendix A. Neglecting the anticoincidental contribution that may contribute only around the backscattering direction (for more details, see Subsection 3.1.1 of [1]), one can obtain a simple expression of the second-order scattering coefficient $\sigma_{r,2}$, defined by [1,17]

$$\begin{aligned}\sigma_{r,2}=\frac{1}{\cos\theta_i}\int_{-\pi/2}^{+\pi/2}\int_{-\pi/2}^{+\pi/2}\mathrm{d}\theta_{-,1}\mathrm{d}\theta_{+,1}&|t_{12}(\chi_{ti}^0)g_{12}(\mathbf{k}_i,\mathbf{k}_{-,1};\mathbf{n}_{ti}^0)|^2\frac{p_s(\gamma_{tA_1}^0)}{|\hat{q}_{-,1}-(k_1/k_2)\hat{q}_i|}S_{12}(\boldsymbol{k}_i,\boldsymbol{k}_{-,1}|\gamma_{tA_1}^0)\\ &\times|r_{23}(\chi_{r-,1}^0)f(\boldsymbol{k}_{-,1},\boldsymbol{k}_{+,1};\boldsymbol{n}_{r-,1}^0)|^2\frac{p_s(\gamma_{rB_1}^0)}{|\hat{q}_{+,1}-\hat{q}_{-,1}|}S_{22}(\boldsymbol{k}_{-,1},\boldsymbol{k}_{+,1}|\gamma_{rB_1}^0)\\ &\times|t_{21}(\chi_{t+,1}^0)g_{21}(\boldsymbol{k}_{+,1},\boldsymbol{k}_r;\boldsymbol{n}_{t+,1}^0)|^2\frac{p_s(\gamma_{tA_2}^0)}{|\hat{q}_r-(k_2/k_1)\hat{q}_{+,1}|}S_{21}(\boldsymbol{k}_{+,1},\boldsymbol{k}_r|\gamma_{tA_2}^0).\end{aligned} \quad (2)$$

To obtain physical results for grazing angles for the case with shadow, the configurations of $\theta_{+,1}$ and θ_r (see Fig. 1) that induce local scattering angles greater than $\pi/2$ in absolute values must be omitted. The slopes $\gamma_{tA_1}^0,\gamma_{rB_1}^0,\gamma_{tA_2}^0$ are defined by [1]

$$\gamma_{tA_1}^0=-(k_{-,1}-k_i)/(q_{-,1}-q_i), \quad (3)$$

$$\gamma_{rB_1}^0=-(k_{+,1}-k_{-,1})/(q_{+,1}-q_{-,1}), \quad (4)$$

$$\gamma_{tA_2}^0=-(k_r-k_{+,1})/(q_r-q_{+,1}). \quad (5)$$

$t_{\alpha\beta}$ is the transmission Fresnel coefficient from the medium Ω_α into the medium Ω_β; f and $g_{\alpha\beta}$ are projection terms; and

$$S_{12}(\boldsymbol{k}_i,\boldsymbol{k}_{-,1}|\gamma_{tA_1}^0),\ S_{22}(\boldsymbol{k}_{-,1},\boldsymbol{k}_{+,1}|\gamma_{rB_1}^0),\ S_{21}(\boldsymbol{k}_{+,1},\boldsymbol{k}_r|\gamma_{tA_2}^0)$$

are the bistatic shadowing functions in transmission from the medium Ω_1 into the medium Ω_2, in reflection inside the medium Ω_2 and onto the medium Ω_3, and in transmission from the medium Ω_2 back into the medium Ω_1, respectively [7,8].

Thus, the problem can be reduced to only twofold integrations, which enables a fast numerical implementation. One can observe that under the GOA, expression (2) can be applied for any given slope statistics and is independent of the frequency and of the surface height statistics (within the validity domain of the model). Moreover, assuming that the points of successive scattering A_1, B_1, and A_2 (see Fig. 1; this assumption will be discussed later) are uncorrelated, this expression appears as the product of three elementary scattering coefficients of single interfaces (which we will denote $s_{t,12}^{A_1}$, $s_{r,23}^{B_1}$, and $s_{t,21}^{A_2}$), each one corresponding to each scattering in reflection or transmission inside the rough dielectric waveguide. Indeed, the first one, $s_{t,12}^{A_1}$, defined by

$$s_{t,12}^{A_1}=|t_{12}(\chi_{ti}^0)g_{12}(\boldsymbol{k}_i,\boldsymbol{k}_{-,1};\boldsymbol{n}_{ti}^0)|^2\frac{p_s(\gamma_{tA_1}^0)}{|\hat{q}_{-,1}-(k_1/k_2)\hat{q}_i|}\times S_{12}(\boldsymbol{k}_i,\boldsymbol{k}_{-,1}|\gamma_{tA_1}^0), \quad (6)$$

corresponds to the scattering in transmission from point A_1 of Σ_A into the medium Ω_2; the second one, $s_{r,23}^{B_1}$, defined by

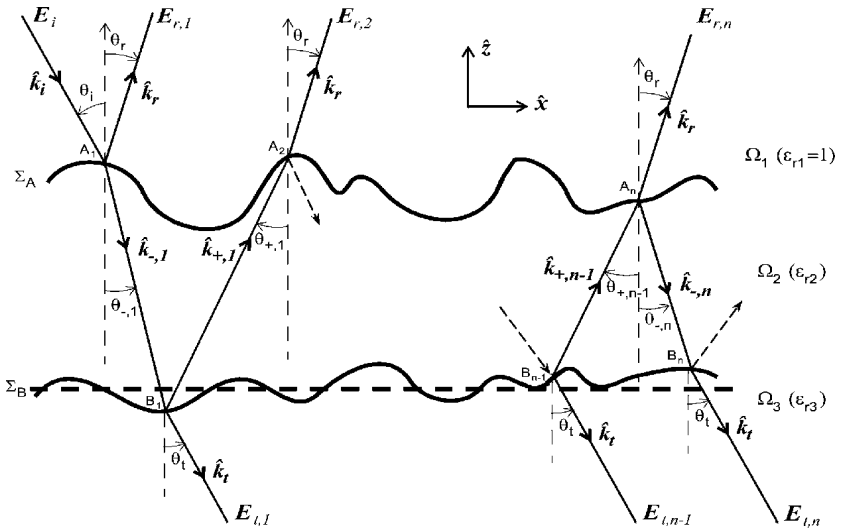

Fig. 1. Multiple scattering from a rough layer. The points on the upper surface Σ_A are denoted as $\{A_1, A_2, \ldots, A_n\}$, whereas the points on the lower surface Σ_B are denoted as $\{B_1, B_2, \ldots, B_n\}$; θ_i is the incidence angle, and θ_r, θ_t are the scattering angles in reflection and transmission, respectively, measured with respect to the vertical axis $\hat{\mathbf{z}}$. The positive sense is defined as clockwise.

$$s_{r,23}^{B_1} = |r_{23}(\chi_{r-,1}^0) f(\boldsymbol{k}_{-,1}, \boldsymbol{k}_{+,1}; \boldsymbol{n}_{r-,1}^0)|^2 \times \frac{p_s(\gamma_{rB_1}^0)}{|\hat{q}_{+,1} - \hat{q}_{-,1}|} S_{22}(\boldsymbol{k}_{-,1}, \boldsymbol{k}_{+,1} | \gamma_{rB_1}^0), \tag{7}$$

corresponds to the scattering in reflection from point B_1 of Σ_B inside Ω_2; and the third one, $s_{t,21}^{A_2}$, defined by

$$s_{t,21}^{A_2} = |t_{21}(\chi_{t+,1}^0) g_{21}(\boldsymbol{k}_{+,1}, \boldsymbol{k}_r; \boldsymbol{n}_{t+,1}^0)|^2 \times \frac{p_s(\gamma_{tA_2}^0)}{|\hat{q}_r - (k_2/k_1)\hat{q}_{+,1}|} S_{21}(\boldsymbol{k}_{+,1}, \boldsymbol{k}_r | \gamma_{tA_2}^0), \tag{8}$$

corresponds to the scattering in transmission from point A_2 of Σ_A back into the medium Ω_1.

Thus, $\sigma_{r,2}$ can be expressed as

$$\sigma_{r,2}(\theta_r, \theta_i) = \frac{1}{\cos\theta_i} \iint \mathrm{d}\theta_{-,1} \mathrm{d}\theta_{+,1} s_{t,12}^{A_1} s_{r,23}^{B_1} s_{t,21}^{A_2}. \tag{9}$$

The twofold integrals account for the energy spread by the rough surfaces in all scattering directions.

Using the exact same method as for $\sigma_{r,1}$ and $\sigma_{r,2}$, one can obtain the expression of the first-order transmission scattering coefficient $\sigma_{t,1}$. Thus, $\sigma_{t,1}$ is defined by [1]

$$\sigma_{t,1}(\theta_t, \theta_i) = \sqrt{\frac{\epsilon_{r3}}{\epsilon_{r1}}} \frac{1}{\cos\theta_i} \int_{-\pi/2}^{+\pi/2} \mathrm{d}\theta_{-,1} |t_{12}(\chi_{ti}^0) g_{12}(\boldsymbol{k}_i, \boldsymbol{k}_{-,1}; \boldsymbol{n}_{ti}^0)|^2 \times \frac{p_s(\gamma_{tA_1}^0)}{|\hat{q}_{-,1} - (k_1/k_2)\hat{q}_i|} S_{12}(\boldsymbol{k}_i, \boldsymbol{k}_{-,1} | \gamma_{tA_1}^0) \times |t_{23}(\chi_{t-,1}^0) g_{23}(\boldsymbol{k}_{-,1}, \boldsymbol{k}_t; \boldsymbol{n}_{t-,1}^0)|^2 \times \frac{p_s(\gamma_{tB_1}^0)}{|\hat{q}_t - (k_2/k_3)\hat{q}_{-,1}|} S_{23}(\boldsymbol{k}_{-,1}, \boldsymbol{k}_t | \gamma_{tB_1}^0). \tag{10}$$

As for using elementary scattering coefficients, $\sigma_{r,2}$, $\sigma_{t,1}$ can be expressed as

$$\sigma_{t,1}(\theta_t, \theta_i) = \frac{1}{\cos\theta_i} \int \mathrm{d}\theta_{-,1} s_{t,12}^{A_1} s_{t,23}^{B_1}, \tag{11}$$

with

$$s_{t,23}^{B_1} = |t_{23}(\chi_{t-,1}^0) g_{23}(\boldsymbol{k}_{-,1}, \boldsymbol{k}_t; \boldsymbol{n}_{t-,1}^0)|^2 \times \frac{p_s(\gamma_{tB_1}^0)}{|\hat{q}_t - (k_2/k_3)\hat{q}_{-,1}|} S_{23}(\boldsymbol{k}_{-,1}, \boldsymbol{k}_t | \gamma_{tB_1}^0). \tag{12}$$

As for $\sigma_{r,2}$, the same concluding remarks can be made on the expression of $\sigma_{t,1}$.

B. Higher Orders of Reflection and Transmission Scattering Coefficients

The preceding expressions of scattering coefficients can easily be extended to any order of scattering from the rough layer, in reflection as well as in transmission. This step can be understood using elementary scattering coefficients corresponding to each scattering point in reflection or transmission inside the rough layer.

Let us define the following general elementary scattering coefficients:

$$s_{r,12}^{A_1} \equiv \cos\theta_i \sigma_{r,1} = |r_{12}(\chi_{ri}^0) f(\boldsymbol{k}_i, \boldsymbol{k}_r; \boldsymbol{n}_{ri}^0)|^2 \frac{p_s(\gamma_{ri}^0)}{|\hat{q}_r - \hat{q}_i|} S_{11}(\boldsymbol{k}_i, \boldsymbol{k}_r | \gamma_r^0), \tag{13}$$

$$s_{r,23}^{B_m} = |r_{23}(\chi_{r-,m}^0) f(\boldsymbol{k}_{-,m}, \boldsymbol{k}_{+,m}; \boldsymbol{n}_{r-,m}^0)|^2 \times \frac{p_s(\gamma_{rB_m}^0)}{|\hat{q}_{+,m} - \hat{q}_{-,m}|} S_{22}(\boldsymbol{k}_{-,m}, \boldsymbol{k}_{+,m} | \gamma_{rB_m}^0), \tag{14}$$

$$s_{t,23}^{B_n} = |t_{23}(\chi_{t-,n}^0) g_{23}(\boldsymbol{k}_{-,n}, \boldsymbol{k}_t; \boldsymbol{n}_{t-,n}^0)|^2 \times \frac{p_s(\gamma_{tB_n}^0)}{|\hat{q}_t - (k_2/k_3)\hat{q}_{-,n}|} S_{23}(\boldsymbol{k}_{-,n}, \boldsymbol{k}_t | \gamma_{tB_n}^0), \tag{15}$$

$$s_{r,21}^{A_m} = |r_{21}(\chi_{t+,m-1}^0) f(\boldsymbol{k}_{+,m-1}, \boldsymbol{k}_{-,m}; \boldsymbol{n}_{r+,m-1}^0)|^2 \times \frac{p_s(\gamma_{rA_m}^0)}{|\hat{q}_{-,m} - \hat{q}_{+,m-1}|} S_{22}(\boldsymbol{k}_{+,m-1}, \boldsymbol{k}_{-,m} | \gamma_{rA_m}^0), \quad (16)$$

$$s_{t,21}^{A_n} = |t_{21}(\chi_{t+,n-1}^0) g_{21}(\boldsymbol{k}_{+,n-1}, \boldsymbol{k}_r; \boldsymbol{n}_{t+,n-1}^0)|^2 \times \frac{p_s(\gamma_{tA_n}^0)}{|\hat{q}_r - (k_2/k_1)\hat{q}_{+,n-1}|} S_{21}(\boldsymbol{k}_{+,n-1}, \boldsymbol{k}_r | \gamma_{tA_n}^0). \quad (17)$$

Then one obtains

$$\sigma_{r,1}(\theta_r, \theta_i) = \frac{1}{\cos\theta_i} s_{r,12}^{A_1}, \quad (18)$$

$$\sigma_{t,1}(\theta_t, \theta_i) = \frac{1}{\cos\theta_i} \int \mathrm{d}\theta_{-,1} s_{t,12}^{A_1} s_{t,23}^{B_1}, \quad (19)$$

$$\sigma_{r,2}(\theta_r, \theta_i) = \frac{1}{\cos\theta_i} \int\int \mathrm{d}\theta_{-,1} \mathrm{d}\theta_{+,1} s_{t,12}^{A_1} s_{r,23}^{B_1} s_{t,21}^{A_2}, \quad (20)$$

$$\sigma_{t,2}(\theta_t, \theta_i) = \frac{1}{\cos\theta_i} \int\int\int \mathrm{d}\theta_{-,1} \mathrm{d}\theta_{+,1} \mathrm{d}\theta_{-,2} s_{t,12}^{A_1} s_{r,23}^{B_1} s_{r,21}^{A_2} s_{t,23}^{B_2}, \quad (21)$$

and so on, with all propagation angles $\theta_{\pm,m} \in [-\pi/2; +\pi/2]$. Thus, one can express the general expression of $\sigma_{r,n}, \forall n \geqslant 3$ as

$$\sigma_{r,n}(\theta_r, \theta_i) = \frac{1}{\cos\theta_i} \underbrace{\int \cdots \int}_{2(n-1)} \mathrm{d}\theta_{-,1} \mathrm{d}\theta_{+,n} \times \prod_{m=2}^{n-1} (\mathrm{d}\theta_{+,m-1} \mathrm{d}\theta_{-,m} s_{r,21}^{A_m} s_{r,23}^{B_m}) s_{t,12}^{A_1} s_{r,23}^{B_1} s_{t,21}^{A_n}, \quad (22)$$

and the general expression of $\sigma_{t,n}, \forall n \geqslant 2$ as

$$\sigma_{t,n}(\theta_t, \theta_i) = \frac{1}{\cos\theta_i} \underbrace{\int \cdots \int}_{2n-1} \mathrm{d}\theta_{-,n} \times \prod_{m=1}^{n-1} (\mathrm{d}\theta_{-,m} \mathrm{d}\theta_{+,m} s_{r,23}^{B_m} s_{r,21}^{A_{m+1}}) s_{t,12}^{A_1} s_{t,23}^{B_n}. \quad (23)$$

For the case of a perfectly flat lower interface, the expressions of the scattering coefficients are similar and much simpler, as the general term $\int_{-\pi/2}^{+\pi/2} \mathrm{d}\theta_{+,m} s_{r,23}^{B_m}$ is replaced with $|r_{23}(\theta_{-,m})|^2 \delta(\theta_{+,m} - \theta_{-,m})$, and for $\sigma_{t,n}$ the last term $s_{t,23}^{B_n}$ is replaced with $|t_{23}(\theta_{-,n})|^2 \delta[\sin\theta_t - (\epsilon_{r2}/\epsilon_{r3})^{1/2} \sin\theta_{-,n}]$. Then, for this simpler case, $\sigma_{r,2}$ is computed with only one numerical integration, allowing one to obtain results quasi-instantaneously.

As a concluding remark, one can observe that the calculation of the nth-order reflection scattering coefficient $\sigma_{r,n}$ demands $2(n-1)$-fold numerical integrations for a very rough lower interface and $(n-1)$-fold numerical integrations for a flat lower interface. Similarly, the calculation of the nth-order transmission scattering coefficient $\sigma_{t,n}$ demands $(2n-1)$-fold numerical integrations for a rough lower interface and $(n-1)$-fold numerical integrations for a flat lower interface.

In addition, it is similarly worth highlighting that the expressions of the scattering coefficients in reflection or transmission can easily be extended (at least from a mathematical point of view) to any number of uncorrelated rough layers. Indeed, the principle is the same as before: Using elementary scattering coefficients (in reflection or transmission from the considered rough surface), one will be able to express the desired scattering coefficient.

C. Validity Domain and Advantages of the Method

Before presenting the numerical results, let us summarize the assumptions behind the method and their associated validity domains, as well as the advantages of the method.

The method is based on the iteration of the KA at each scattering inside the rough layer. Then the hypothesis associated with the KA applies here on all the rough surfaces. That is to say, one has the following restriction for an incident wave inside a medium Ω_α onto a rough surface Σ_M [2,3,18,19]:

$$k_\alpha p_M \cos^3\chi_{i,\alpha} \gg 1, \quad (24)$$

with k_α the wavenumber inside Ω_α, p_M the local curvature radius of Σ_M, and $\chi_{i,\alpha}$ the local incidence angle with respect to the local normal to Σ_M. This corresponds to the fact that the surface can be assimilated, locally, to an infinite plane surface. Thus, this method is also called the tangent plane approximation, and denoted TPA, or the Kirchhoff tangent plane approximation, and denoted KTPA (as shown in [20], the KA differs rigorously from the TPA for dielectric surfaces; nevertheless, here this assimilation is made as most authors do). This local criterion is usually extended to a global criterion for the whole surface as

$$k_\alpha R_{cM} \cos^3\theta_{i,\alpha} \gg 1, \quad (25)$$

with R_{cM} the mean curvature radius of Σ_M and $\theta_{i,\alpha}$ the incidence angle inside Ω_α with respect to the vertical axis $\hat{\mathbf{z}}$. Then one obtains here

$$k_1 R_{cA} \cos^3\theta_i \gg 1, \quad \text{and} \quad k_2 R_{cA} \cos^3\theta_{+,m} \gg 1, \quad (26)$$

for a perfectly flat lower interface, plus

$$k_2 R_{cB} \cos^3\theta_{-,m} \gg 1, \quad (27)$$

for a rough lower interface. For Gaussian height PDF and Gaussian height correlation, R_c can be evaluated for small slopes by the approximate expression [21]

$$R_{cM} \simeq \frac{L_{cM}^2}{2.76\sigma_{hM}} \times \left(1 + \frac{3}{2}\frac{\sigma_{hM}^2}{L_{cM}^2}\right), \quad (28)$$

with σ_{hM}, L_{cM} the considered surface root-mean-square (RMS) height and correlation length, respectively. Several authors [21,22] presented more general expressions of the statistical average of the surface curvature radius, $R_{cM} = \langle p_M \rangle$ in order to better evaluate the validity domain of

the KA. One must rigorously study the statistical average over the whole quantity $p_M \cos^3 \chi_{i,\alpha}$.

To be specific on the KA, in this paper only single scattering from the same interface is taken into account; i.e., multiple scattering from a single interface effect [23–25] is not taken into account. Then only the first-order KA (denoted as KA1) is considered here, which reduces the validity domain to gentle rough surfaces, i.e., to small-to-moderate RMS surface slopes, $\sigma_s \lesssim 0.3$ [25–29].

Then, based on the iteration of KA1 (IKA1) for each scattering inside the rough layer, the method is reduced to the high-frequency limit, using the GOA for each scattering. Therefore, this method can be denoted as IKA+GOA in general. Under the GOA, it is usually said that the rough surfaces are very rough as compared to the wavelength. More precisely, this restrictive hypothesis is related to the Rayleigh roughness criterion [3,30,31]

$$Ra^M_{r\alpha\beta} = k_\alpha \sigma_{hM} \cos\theta_{i,\alpha} > \pi/C, \tag{29}$$

with $Ra^M_{r\alpha\beta}$ the Rayleigh roughness parameter expressed in reflection from the surface Σ_M inside the medium Ω_α and onto the medium Ω_β, and C a constant, which is usually taken between 2 and π. Indeed, for a Gaussian height distribution, the coherent reflection power loss $\mathcal{A}_{coh}$ in the KA is given by (see, for instance, Subsection 2.B of [32])

$$\mathcal{A}_{coh} = \exp(-g^2), \tag{30}$$

with $g = 2Ra^M_{r\alpha\beta}$, which leads for $C=\pi$ to $\mathcal{A}_{coh} < -17.4$ dB and for $C=2$ to $\mathcal{A}_{coh} < -42.9$ dB. Let us note that taking $C=1$ and not considering the incidence angle θ_i, which corresponds in vacuum to the commonly written criterion of validity of the GOA (i.e., $\sigma_h \geq \lambda/2$), leads to $\mathcal{A}_{coh} < -171.5$ dB. This criterion is very restrictive. Indeed, as confirmed by the numerical simulation results in [32], one can reasonably take $C=2$ as a general limit of validity. As a consequence, by taking $C=2$, the criterion of validity of the GOA should rather be expressed as

$$\sigma_{hM} \gtrsim \frac{\lambda^{app}_\alpha(\theta_i)}{4}, \tag{31}$$

with $\lambda^{app}_\alpha(\theta_i) = \lambda_\alpha/\cos\theta_i$, which can be seen as a wavelength apparent along the normal to the mean surface [33].

Nevertheless, even though calculating $\mathcal{A}_{coh}$ can give an idea of the validity of neglecting the coherent power, first one must keep in mind that this remains a *qualitative* criterion. Indeed, the GOA is valid if the coherent scattered power is negligible in comparison with the incoherent scattered power (one can find in Appendix B the calculation of the coherent scattering coefficient from a single rough interface under the KA1). Then rigorously calculating the coherent scattered power and comparing it with the incoherent scattered power allows one to determine the effective validity domain of the method. Second, as shown in [9,31], this classical Rayleigh roughness criterion is valid only in the case of reflection onto the considered surface. Then, for the case of transmission through a rough surface Σ_M from the medium Ω_α into the medium Ω_β, the Rayleigh roughness parameter $Ra^M_{t\alpha\beta}$ becomes [31,9]

$$Ra^M_{t\alpha\beta} = k_0 \sigma_{hM} \frac{|n_\alpha \cos\theta_{i,\alpha} - n_\beta \cos\theta_{t,\beta}|}{2} > \pi/C, \tag{32}$$

with n_α the refractive index of the incident medium Ω_α, n_β the refractive index of the transmission medium Ω_β, and $\theta_{t,\beta}$ the angle of transmission inside Ω_β. Here $\theta_{t,\beta}$ is related to $\theta_{i,\alpha}$ by the Snell–Descartes law $n_1 \sin\theta_{i,\alpha} = n_2 \sin\theta_{t,\beta}$ (corresponding to a perfectly flat surface).

This approach, valid for a single rough interface, can be extended to the case of rough layers. Then, as shown in Section 3 of [31], a Rayleigh roughness parameter in reflection $Ra_{r,n}$ and in transmission $Ra_{t,n}$ can be associated to each order n of scattering from the rough layer (see Fig. 1) in order to define a *qualitative* criterion of applicability of the IKA+GOA for each scattering order n. Thus, for uncorrelated rough surfaces, one obtains $Ra_{r,1} = Ra^A_{r12}$, $Ra^2_{t,1} = (Ra^A_{t12})^2 + (Ra^B_{t23})^2$, and $\forall n \geq 2$:

$$Ra^2_{r,n} = 2(Ra^A_{t12})^2 + (n-1)(Ra^B_{r23})^2 + (n-2)(Ra^A_{r21})^2, \tag{33}$$

$$Ra^2_{t,n} = (Ra^A_{t12})^2 + (Ra^B_{t23})^2 + (n-1)[(Ra^B_{r23})^2 + (Ra^A_{r21})^2], \tag{34}$$

the angles of propagation being θ_i inside Ω_1, θ_2 given by $n_1 \sin\theta_i = n_2 \sin\theta_2$ inside Ω_2, and θ_3 given by $n_2 \sin\theta_2 = n_3 \sin\theta_3$ inside Ω_3. For the case of a flat lower interface, the Rayleigh roughness parameters $Ra^B_{t23} = Ra^B_{r23} = 0$. For a rough lower interface, one can notice for $\epsilon_{r2} > \epsilon_{r1}$ that $Ra^B_{r23} > Ra^A_{r12}$. As a consequence, $Ra_{r,2} > Ra_{r,1}$, and the higher orders being superior to $Ra_{r,2}$, one has

$$\forall n \geq 2, \quad Ra_{r,n+1} > Ra_{r,n} > Ra_{r,1}. \tag{35}$$

One must note that these results are obtained under the hypothesis of uncorrelated surfaces, which is the hypothesis under which the scattering coefficients were derived. One can find in Appendix C the expressions of the coherent scattering coefficients $\sigma^{coh}_{t,1}$ and $\sigma^{coh}_{r,2}$, which give a *quantitative* criterion of applicability of the IKA+GOA.

Considering uncorrelated surfaces implies a restriction on the mean layer thickness $\bar{H}$. Indeed, from a physical point of view, the two surfaces do not have to cross each other, which implies for a flat lower interface the following statistical criterion (for Gaussian height PDF): $\bar{H} \gtrsim 4\sigma_{hA}$. Similarly, for a rough lower interface, it would imply the statistical criterion $\bar{H} \gtrsim 4(\sigma_{hA} + \sigma_{hB})$. Nevertheless, as the two surfaces obey independent statistical processes, the constraint can be reduced to, let us say, $\bar{H} \gtrsim 3(\sigma_{hA} + \sigma_{hB})$. Moreover, the method assumes that the points of successive scattering inside the rough layer are uncorrelated between one another, which could reduce its applicability for uncorrelated surfaces to slightly larger thicknesses. Nevertheless, this supplementary restriction on the layer thickness is not significant: The first condition implies in practice the second one.

Moreover, in the calculation of the second-order scattering coefficient (as well as for higher orders), the anticoincidental contribution (which occurs only around the backscattering direction) was neglected, which restricts the

applicability of the method to layer thicknesses $\bar{H}$ obeying [1,34] (at least for a flat lower interface)

$$\bar{H} < \frac{\sqrt{\epsilon_{r2}}}{\sqrt{\epsilon_{r2}} - \sqrt{\epsilon_{r1}}} R_{cA}, \tag{36}$$

with R_{cA} the mean curvature radius of the upper interface.

As written previously, the model can take lossless as well as lossy media into account. Still, one can notice that the expressions of the scattering coefficients are independent of the layer mean thickness $\bar{H}$ (neglecting the anticoincidental case), which means that the model itself cannot determine a layer thickness. This corresponds to the use of the GOA, in which the phase term is not taken into account (the phase being uniformly distributed between $-\pi$ and $+\pi$). Thus, the model itself cannot deal with lossy inner media (Ω_2, with $\epsilon_{r2} \equiv \epsilon_{r2} \in \mathbb{C} \setminus \mathbb{R}$). Nevertheless, it was shown in Section 7 of [1] that making minor adjustments to the model allows one to deal with lossy media with good accuracy.

In particular, the propagation loss $\mathcal{A}_{r,2}$ of the second-order scattering coefficient in reflection $\sigma_{r,2}$ can be evaluated for a Gaussian height distribution and by considering flat interfaces, $\mathcal{A}_{r,2}^{pl}$. It is then given approximately by [1]

$$\mathcal{A}_{r,2} \simeq \mathcal{A}_{r,2}^{pl} = \exp(-4k_0 q \bar{H}/\cos\theta_{m,1}^{\text{plane}}). \tag{37}$$

Then the propagation loss $\mathcal{A}_{r,n}$ associated with the nth-order scattering coefficient in reflection $\sigma_{r,n}$ is given by $\mathcal{A}_{r,n} = (\mathcal{A}_{r,2})^{n-1}$, with $n \geq 2$. Similarly, the propagation loss $\mathcal{A}_{t,1}$ associated with the first-order scattering coefficient in transmission $\sigma_{t,1}$ is given by $\mathcal{A}_{t,1} = (\mathcal{A}_{r,2})^{1/2}$. Thus, the propagation loss $\mathcal{A}_{t,n}$ associated with the nth-order scattering coefficient in transmission $\sigma_{t,n}$ is given by $\mathcal{A}_{t,n} = (\mathcal{A}_{r,2})^{n-1/2}$, with $n \geq 1$.

One last condition deals with the applicability of the geometric shadowing functions used (which, strictly speaking, are valid only for monoscale rough surfaces). They do not take the penumbra effect [35] into account, which, in practice, contributes for very low grazing angles [see Eq. (18) of [35]]. Indeed, for the typical applications presented here, the geometric shadowing functions can be applied with good approximations up to scattering angles of the order of 85–87 deg in absolute value [1].

In summary, the validity domains of the method are given by the following conditions:

1. KA: $k_1 R_{cA} \cos^3\theta_i \gg 1$ and $k_2 R_{cA} \cos^3\theta_{+,m} \gg 1$ for a flat lower interface, plus $k_2 R_{cB} \cos^3\theta_{-,m} \gg 1$ for a rough lower interface.
2. KA1: $\sigma_s \lesssim 0.3$.
3. GOA: Great layer electromagnetic roughness $\{Ra_{r,n}, Ra_{t,n}\} > \pi/C$, with $C \approx 2$, so that the incoherent scattering coefficient equals the scattering coefficient (the coherent scattering coefficient being neglected).
4. U-IKA (uncorrelated surfaces): $\bar{H} \gtrsim 4\sigma_{hA}$ for a flat lower interface, $\bar{H} \gtrsim 3(\sigma_{hA} + \sigma_{hB})$ for a rough lower interface.
5. Neglecting the anticoincidental contribution: $\bar{H} < \frac{\sqrt{\epsilon_{r2}}}{\sqrt{\epsilon_{r2}} - \sqrt{\epsilon_{r1}}} R_{cA}$.
6. Applicability of shadowing functions: scattering angles $|\theta_r| \lesssim 87°$.

The main advantages of the method can be listed as follows:

- It is independent of the height distribution and of the frequency (at least for lossless media and when the anticoincidental contribution can be neglected).
- It can deal with any given slope distribution.
- It can deal with lossless as well as lossy media.
- It can treat very rough or perfectly flat lower interfaces.
- It is easy to implement, robust, and fast in computation.

3. IMPLEMENTATION AND NUMERICAL RESULTS

A. Numerical Implementation

It is possible to optimize the method's computing time, which is directly related to the number of sampling points in the numerical integrations to calculate. That is to say, in general it is not necessary to integrate over the propagation angles $\theta_{\pm,m}$ in the whole range $[-\pi/2; +\pi/2]$, as some values of propagation angles have a very low contribution. Under the IKA+GOA, the scattering coefficient appears as the product of elementary scattering coefficients corresponding to each scattering inside the rough layer. Each scattering coefficient is proportional to the considered surface slope distribution, which plays a major role in the scattering coefficient σ. Then, as a first approximation, one can consider only the slope distribution in the expression of σ in order to delimit the effective contributing range of the scattering coefficient over the propagation angles $\theta_{\pm,m}$.

By considering the limit angles $\theta_{\pm,m}^{min}$, $\theta_{\pm,m}^{max}$ corresponding to a surface slope $\gamma_M = \pm n_M \sigma_{sM}$, with σ_{sM} the RMS surface slope of considered surface and n_M a real number to be chosen (which is typically taken between 3 and 4 for a Gaussian distribution), one can estimate the corresponding limit propagation angles. Indeed, the local incidence angle $\chi_{i,\alpha}$ is given by

$$\chi_{i,\alpha} = \theta_{i,\alpha} + \arctan\gamma_M. \tag{38}$$

Then the scattering angles in reflection $\theta_{r,\alpha}$ and in transmission $\theta_{t,\alpha}$ are given by

$$\theta_{r,\alpha} = -\chi_{i,\alpha} - \arctan\gamma_M = -\theta_{i,\alpha} - 2\arctan\gamma_M, \tag{39}$$

$$\theta_{t,\alpha} = \arcsin\left[\sqrt{\frac{\epsilon_{r1}}{\epsilon_{r2}}}\sin\chi_{i,\alpha}\right] - \arctan\gamma_M, \tag{40}$$

respectively. Thus, $\theta_{r,\alpha}^{min}$ and $\theta_{t,\alpha}^{min}$ are given by $\gamma_M = +n_M\sigma_{sM}$, and $\theta_{r,\alpha}^{max}$ and $\theta_{t,\alpha}^{max}$ are given by $\gamma_M = -n_M\sigma_{sM}$.

In the next subsection, numerical results of the incoherent scattering coefficient from different rough layers, with various configurations, are presented first for a rough layer with a rough lower interface, and second for a perfectly flat lower interface. The results are computed for homogeneous media, with $\epsilon_{r2} = 3$ and $\epsilon_{r3} = i\infty$ (the upper medium being the air, assimilated to vacuum, so that $\epsilon_{r1} = 1$). The surface RMS slope is taken as $\sigma_{sA} = \sigma_{sB} = 0.1$. The incident wave has V polarization. The influence of the

mean layer thickness $\bar{H}$ and of the surface RMS heights σ_{hA} and σ_{hB} will be studied in order to check whether they influence the scattering coefficient and to check conditions 4 and 5 on $\bar{H}$ and especially condition 3 on σ_{hA} and σ_{hB}.

The results of the total scattering coefficient $\sigma_{r,n}^{tot} = \Sigma_{k=1}^{n} \sigma_{r,k}$ from the IKA+GOA are plotted by comparison with the reference numerical method, namely, the PILE method [10] accelerated by the FB-SA [11], for different orders of scattering. The numerical parameters of the PILE method are the surface length $L_0 = L_A = L_B = 400\lambda$, the number of sampling points of each interface $n_i = 4000$, the number of realizations of the Monte Carlo process $N = 70$, and the attenuation parameter of the incident Thorsos wave $g = L_0/6$. The forward-backward method is used at order 8 for the upper surface and at order 2 for the lower interface, and the spectral acceleration is computed with a distance of strong interactions equal to three times the surface correlation length (which makes it at least 8.5 electromagnetic (EM) wavelengths in free space for all simulations presented here for a rough lower interface, and equal to 7.1 EM wavelengths in free space for the simulation presented here for a flat lower interface).

B. Numerical Results for a Rough Lower Interface

First, numerical results of the incoherent scattering coefficient are presented for a rough lower interface. Figure 2 presents results for a mean layer thickness $\bar{H} = 6\lambda$, and the two surfaces Σ_A and Σ_B have the same statistical parameters: The surface RMS height $\sigma_{hA} = \sigma_{hB} = 0.2\lambda$ (the surface RMS slope being $\sigma_{sA} = \sigma_{sB} = 0.1$). The incident wave (of V polarization) has an incidence angle $\theta_i = 0°$. The results from the IKA+GOA are plotted by comparison with the reference numerical method, namely, the PILE +FB-SA, for different orders of scattering.

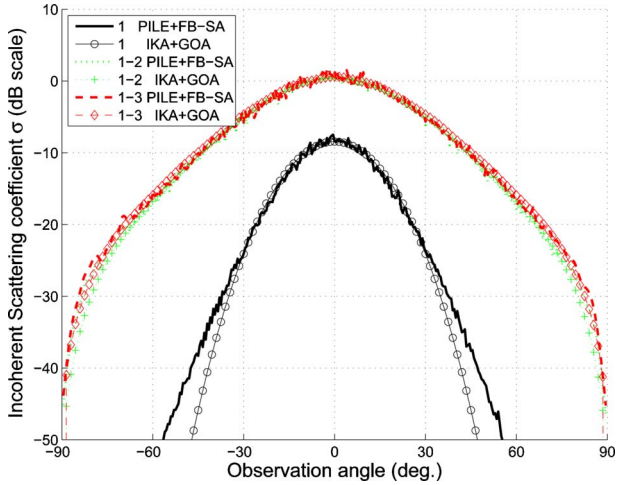

Fig. 2. (Color online) Simulations of the contributions of the first three orders of the total incoherent scattering coefficient $\sigma_{r,n}^{tot}$ (in decibel scale) versus the observation angle θ_r (in degrees) for V polarization and $\theta_i = 0°$, with $\bar{H} = 6\lambda$, for relative permittivities $\epsilon_{r2} = 3$ and $\epsilon_{r3} = i\infty$, and the surface RMS slope $\sigma_{sA} = \sigma_{sB} = 0.1$. For both surfaces, the surface RMS height $\sigma_{hA} = \sigma_{hB} = 0.2\lambda$. In the legend, the numerical reference method is denoted as PILE +FB-SA, and the asymptotic method as IKA+GOA.

Concerning the first-order incoherent scattering coefficient, which corresponds to the scattering from only the surface Σ_A, there is a good agreement between the IKA +GOA and the reference method. The differences for scattering angles $|\theta_r|$ greater than 40°, which have low contributions (less than −30 dB), can be attributed to the contributions of multiple scattering (mainly double scattering) from the interface. The contribution of the *coherent* first-order scattering coefficient of the reference method is plotted in Fig. 3 for comparison. One can observe a sharp enhancement of its contribution in the specular direction, whose level is approximately 5.6 dB lower than the incoherent contribution. In this case, the reflection Rayleigh roughness parameter $Ra_{r12}^{A} = k_1 \sigma_{hA} \cos\theta_i \simeq 1.26$, and thus the reflection Rayleigh roughness (qualitative) criterion $Ra_{r12}^{A} > \pi/C$, with $C = 2$, is not strictly valid. Nevertheless, it is close to the limit of validity, which is confirmed by the numerical results. Indeed, a 5.6 dB difference is not sufficient to consider that the coherent component can be neglected, but its contribution is low. Then, for a bit higher values of RMS heights, the criterion will be valid: For instance, for $\sigma_{hA} = 0.25\lambda$, numerical results not presented here show that the coherent component is at least 15 dB inferior to the incoherent component.

For the higher-order contributions of the scattering coefficient, first, the second-order contribution highlights a very good agreement between the IKA+GOA and the reference method in all scattering directions. Only small differences appear for grazing scattering angles $|\theta_r| \gtrsim 80°$, which can be attributed to the contribution of multiple scattering from the same interface (moreover, for $|\theta_r| \gtrsim 87°$ the IKA+GOA using geometrical shadowing functions begins not to be valid any more). Furthermore, one can see in Fig. 3 that the coherent contribution in the specular direction is approximately 12 dB lower than the incoherent contribution, which means that in this configuration the coherent contribution can be neglected: The IKA+GOA can be applied to determine the scattering coefficient, which can be assimilated to the *incoherent* scattering coefficient. The latter result differs from that of the

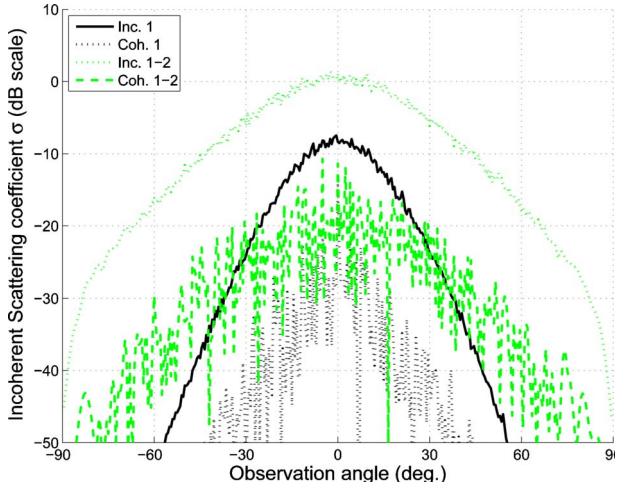

Fig. 3. (Color online) Same simulation parameters as in Fig. 2: Comparison of the incoherent and coherent contributions of the PILE+FB-SA numerical reference method for the first- and second-order contributions.

first-order contribution, where the difference was not so significant. This can be understood by the calculation of the Rayleigh roughness parameter associated with this scattering coefficient, $Ra_{r,2}=[2(Ra_{t12}^{A})^2+(Ra_{r23}^{B})^2]^{1/2}$. It is composed of twice the elementary Rayleigh parameter in transmission from the upper interface, Ra_{t12}^{A}, and the elementary Rayleigh parameter in reflection from the lower interface, Ra_{r23}^{B}. Note that Ra_{r23}^{B} is in general superior to Ra_{r12}^{A} for $\sigma_{hB}=\sigma_{hA}$ and $k_2 \geqslant k_1$. Here, as $\theta_i=0$, $Ra_{r23}^{B}=\sqrt{\epsilon_{r2}}Ra_{r12}^{A}$ and equals $Ra_{r23}^{B}\simeq 2.18>\pi/2$, which means that the coherent contribution can be neglected. Moreover, as $Ra_{t}^{A}=(\sqrt{\epsilon_{r2}}-1)/2\times Ra_{r12}^{A}$, which equals $Ra_{t12}^{A}\simeq 0.46$, the Rayleigh roughness parameter associated with the second-order scattering coefficient $Ra_{r,2}\simeq 2.27>\pi/2$. Because the first-order contribution $\sigma_{r,1}$ is negligible against the second-order contribution $\sigma_{r,2}$ in the total second-order contribution $\sigma_{r,2}^{tot}=\sigma_{r,1}+\sigma_{r,2}$, this qualitative criterion is then in agreement with the numerical results. This is an interesting result, because for a rough lower interface, it means that even though in the case of the upper interface alone, the Rayleigh roughness criterion $Ra_{r,1}=Ra_{r12}^{A}$ is not superior to $\pi/2$ (which means that the coherent contribution cannot be neglected in comparison with the incoherent contribution, corresponding to the applicability of the GOA), it can be the case for the whole system, because the higher-order Rayleigh parameters $Ra_{r,n}>Ra_{r,1}$ (with $n\geqslant 2$). It is the case here, which means that for such a configuration, the IKA+GOA can be applied to lower RMS surface heights σ_h than previously expected—at least down to 0.2λ when $\sigma_{hA}=\sigma_{hB}$.

The third-order scattering coefficient $\sigma_{r,3}$ contributes very weakly to the total scattering coefficient $\sigma_{r,3}^{tot}=\sigma_{r,1}+\sigma_{r,2}+\sigma_{r,3}$, and only for grazing θ_r. The results of $\sigma_{r,3}^{tot}$ from the IKA+GOA differ from the second-order contribution $\sigma_{r,2}^{tot}$ only for grazing scattering angles, and the same conclusions can be drawn. Then the higher-order contributions can be neglected. Similarly, because the coherent total contribution is of the same order as the one of the second-order scattering coefficient, it can be neglected. Thus, for this configuration, the calculation of the first three orders of the scattering coefficient is sufficient in order to quantify the scattering from such a system. The IKA+GOA gives good agreement with the reference method in such a case. This method is then an interesting means to quickly compute the total scattering coefficient. Indeed, by using the optimization described in Subsection 3.A, the results were obtained in only 4 ms for $\sigma_{r,2}^{tot}$ and in 1.5 s for $\sigma_{r,3}^{tot}$ for given θ_i and θ_r (with 6, 15, 31, and 21 sampling points for the numerical integrations over $\theta_{-,1}$, $\theta_{+,1}$, $\theta_{-,2}$, and $\theta_{+,2}$, respectively) with a standard personal computer (2.33 GHz biprocessor, 1.96 GB RAM) using MatLab. The computing time for the PILE+FB-SA reference method on the same computer is of the orders of 11, 14.5, and 21 min for PILE up to orders 3, 4, and 6, respectively, for each realization, which makes 13, 17, and 25 h, respectively, for 70 realizations. One property of the IKA+GOA is that under the GOA, the phase of the total scattered field on the upper surface is uniformly distributed between $-\pi$ and $+\pi$. For all configurations studied here, results from the reference method allowed us to check this property.

Figure 4 presents results for the same parameters as in Fig. 2, except for $\theta_i=-5°$, $\bar{H}=5\lambda$ and different RMS surface heights $\sigma_{hA}=0.35\lambda$, $\sigma_{hB}=0.25\lambda$. The results from the first-order scattering coefficient $\sigma_{r,1}^{tot}=\sigma_{r,1}$ of the IKA+GOA are in very good agreement with the reference method, and the small differences (with very low levels) that appear away from the specular direction can be attributed to the multiple scattering effect. Moreover, the coherent contribution is approximately 12 dB lower than the incoherent one and can be neglected, which means that the GOA is valid. This is confirmed by the first-order Rayleigh roughness criterion $Ra_{r,1}=Ra_{r12}^{A}>\pi/2\simeq 1.57$, as $Ra_{r,1}\simeq 2.19$.

The results from $\sigma_{r,2}^{tot}=\sigma_{r,1}+\sigma_{r,2}$ also highlight a very good agreement between the IKA+GOA and the reference method for all scattering angles θ_r. The small differences (with low levels) that appear for grazing θ_r can be attributed to multiple scattering from the same interface effect. The same observations and conclusions can be drawn for $\sigma_{r,3}^{tot}$. The differences between $\sigma_{r,2}^{tot}$ and $\sigma_{r,3}^{tot}$ are very small and appear only for low contributions at angles $|\theta_r|\gtrsim 60°$. Moreover, the higher-order contributions, $\sigma_{r,n}^{tot}$ (with $n\geqslant 4$), can be neglected. The coherent contributions (not presented here) can be neglected in comparison with the incoherent ones (as $Ra_{r,2}\simeq 2.95>\pi/2$ and $Ra_{r,n}>Ra_{r,2}\ \forall n\geqslant 3$), which validates the IKA+GOA. Comparing these results with the ones in Fig. 2, we conclude that the method can be applied for different mean thicknesses $\bar{H}$ and different RMS surface heights σ_{hA} and σ_{hB} (where σ_{hA} and σ_{hB} can be different). This confirms the theoretical results, which predicted that under conditions 3, 4, and 5, the numerical results are independent of $\bar{H}$, σ_{hA}, and σ_{hB}.

Figure 5 presents simulation results for the same parameters as in Fig. 2, except for $\theta_i=-20°$, $\bar{H}=3\lambda$, and different RMS surface heights $\sigma_{hA}=0.25\lambda$, $\sigma_{hB}=0.35\lambda$. Similar to the preceding two configurations, the first-order contribution $\sigma_{r,1}^{tot}=\sigma_{r,1}$ highlights a good agreement between the IKA+GOA and the reference method, and the same conclusions can be drawn. For the second-order con-

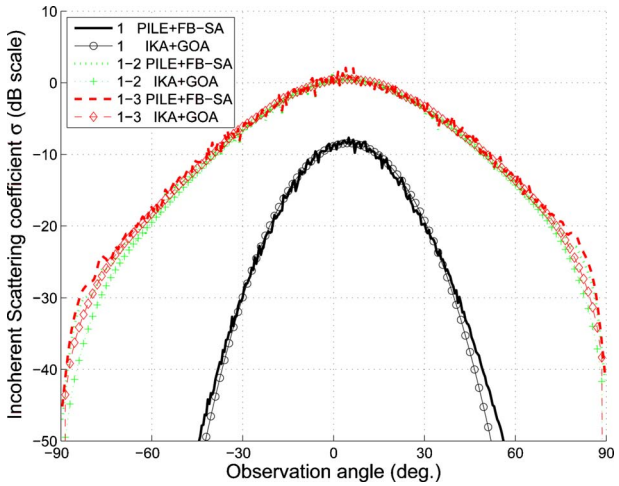

Fig. 4. (Color online) Same simulation parameters as in Fig. 2, but with $\theta_i=-5°$, $\bar{H}=5\lambda$ and different RMS surface heights $\sigma_{hA}=0.35\lambda$, $\sigma_{hB}=0.25\lambda$.

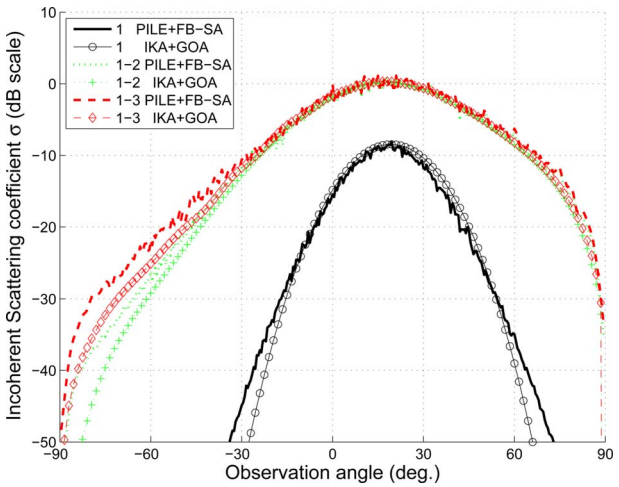

Fig. 5. (Color online) Same simulation parameters as in Fig 2, but with $\theta_i=-20°$, $\bar{H}=3\lambda$, and different RMS surface heights $\sigma_{hA}=0.25\lambda$, $\sigma_{hB}=0.35\lambda$.

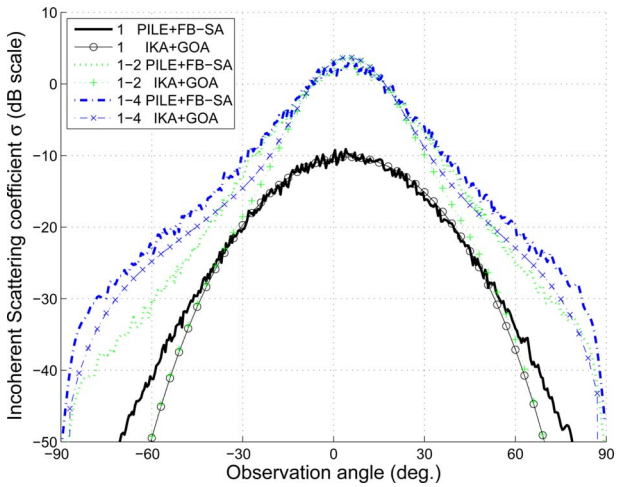

Fig. 6. (Color online) Same simulation parameters as in Fig. 2, but for a perfectly flat lower interface, with $\theta_i=-5°$, $\bar{H}=2\lambda$, $\sigma_{sA}=0.15$, and $\sigma_{hA}=0.25\lambda$. The fourth-order contribution is plotted here for both methods. Then, for the sake of clarity of the figure, the third-order contribution is not represented.

tribution $\sigma_{r,2}^{tot}=\sigma_{r,1}+\sigma_{r,2}$, one can also observe a very good agreement, especially in forward directions (i.e., for $\theta_r>0$). In backward directions $\theta_r<0$, differences appear for $\theta_r<-40°$ and increase when θ_r decreases. The IKA+GOA underestimates the incoherent scattering coefficient, which can be attributed to multiple scattering from the same interface effect (which is not taken into account here in the model). The same observations and conclusions can be drawn for the third-order contribution $\sigma_{r,3}^{tot}=\sigma_{r,1}+\sigma_{r,2}+\sigma_{r,3}$. Then the higher-order scattering coefficients $\sigma_{r,n}, \forall n \geqslant 4$, do not contribute to the total scattering coefficient and can be neglected. Once more, the results confirm that in the validity domain of the IKA+GOA, $\sigma_{r,n}^{tot}$ is independent of $\bar{H}$, σ_{hA}, and σ_{hB}.

C. Numerical Results for a Flat Lower Interface

Figure 6 presents results for the case of a perfectly flat lower interface. The simulation parameters are identical to the ones of Fig. 2, except that $\theta_i=-5°$, $\bar{H}=2\lambda$, $\sigma_{hA}=0.25\lambda$, and $\sigma_{sA}=0.15$. The contribution of the first-order (incoherent) scattering coefficient $\sigma_{r,1}^{tot}=\sigma_{r,1}$ highlights a very good agreement between the IKA+GOA and the reference method around the specular direction. The differences that appear for $\theta_r \lesssim -45°$ and $\theta_r \gtrsim 55°$ can be attributed to multiple scattering from the same interface effect. This effect is a bit higher here than before: Indeed, the multiple scattering effect increases as the surface RMS slope σ_{sA} increases. In Fig. 7, one can observe that the coherent contribution is approximately 14 dB lower than the incoherent one and can thus be neglected. This observed difference is in rather good agreement with the qualitative Rayleigh criterion $Ra_{r,1}>\pi/2$, as the Rayleigh roughness parameter equals $Ra_{r,1}\simeq 1.56\simeq\pi/2$.

The second-order contribution $\sigma_{r,2}^{tot}=\sigma_{r,1}+\sigma_{r,2}$ highlights a good agreement between the IKA+GOA and the reference method only around the specular direction. This can be attributed to multiple scattering from the same interface effect. From Fig. 7, the coherent contribution in the specular direction is approximately 6 dB lower than the incoherent one. This difference is a bit higher than the prediction from the qualitative criterion $Ra_{r,2}>\pi/2$, as here $Ra_{r,2}\simeq 0.81$. This highlights limitations of this qualitative criterion, which is here a bit too restrictive. Nevertheless, for $\theta_i=0°$, this qualitative criterion is valid, as the observed difference is approximately 1 dB, and $Ra_{r,2}\simeq 0.81$. The third-order contribution $\sigma_{r,3}^{tot}$ (which is not represented here for the sake of clarity of the figure) highlights a good agreement between the IKA+GOA and the reference method for all scattering angles. The small differences that appear away from the specular direction can be attributed to multiple scattering from the same interface effect. The same observations and conclusions can be drawn for $\sigma_{r,4}^{tot}$, which, compared to $\sigma_{r,3}^{tot}$, contributes very weakly to the scattering process, and only for grazing θ_r. The higher-order contributions can be neglected here.

Thus, the calculation of the first four orders of the scattering coefficient is enough to quantify the scattering from such a system. As for a rough lower interface, the results do not depend on either $\bar{H}$ or σ_{hA}, which is in agree-

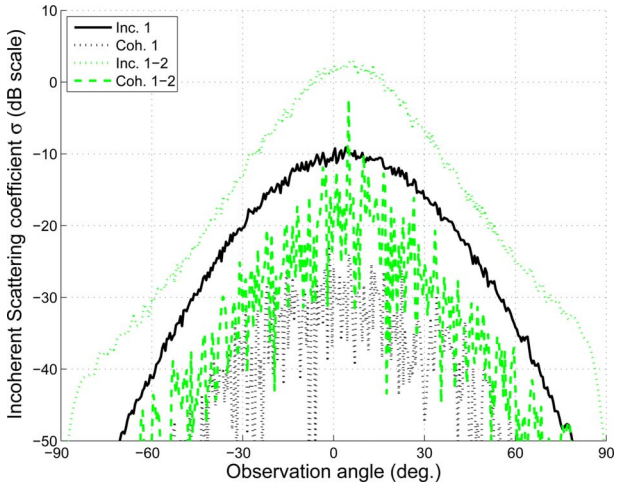

Fig. 7. (Color online) Same simulation parameters as in Fig. 6: Comparison of the incoherent and coherent contributions of the PILE+FB-SA numerical reference method for the first- and second-order contributions.

ment with the predictions of the IKA+GOA. Compared to the rough lower interface, for a flat lower interface the condition of validity on σ_{hA} is a bit more restrictive, as one must have $\sigma_{hA} \gtrsim 0.25\lambda$ (for moderate θ_i).

For lossy inner media, the numerical results (not presented here) highlight a good agreement between the IKA+GOA and the reference method. As shown in Section 7 of [1], taking only the propagation loss [given by Eq. (37) for the second-order contribution] into account allows a good quantification of the losses from the lossy media. In our model, the second-order contribution $\sigma_{r,2}$ is attenuated by the propagation loss factor $\mathcal{A}_{r,2}^{pl}$, and the higher-order terms $\sigma_{r,n}$ $(\forall n \geqslant 3)$ by the factor $\mathcal{A}_{r,n}^{pl} = (\mathcal{A}_{r,2}^{pl})^{n-1}$. Thus, the higher-order terms $\sigma_{r,n}$ will not contribute to the total scattering coefficient, and only the first three orders $\sigma_{r,1}$, $\sigma_{r,2}$, and $\sigma_{r,3}$ (only the first two for a rough lower interface) will be necessary to quantify the scattering phenomenon.

4. CONCLUSION

In conclusion, by using the optimization expressed in Subsection 3.A in the numerical implementation of the IKA+GOA, it is possible to obtain numerical results of the total scattering coefficient that are in very good agreement with those of the reference method. The results are obtained quickly, as the necessary computing time for given θ_i and θ_r is at most 1.5 s with a standard personal computer (2.33 GHz biprocessor, 1.96 GB RAM), using MatLab. For a rough lower interface, as a general rule the first three orders of the scattering coefficient are enough to correctly quantify the scattering phenomenon from the rough layer, and for a plane lower interface, the first four orders are enough.

The numerical results confirmed that under hypotheses 4 and 5, in the validity domain of the IKA+GOA, the results are independent of the mean layer thickness $\bar{H}$ for lossless media. Each scattering coefficient contribution $\sigma_{r,n}^{tot}$ is well quantified by the IKA+GOA. The observed differences with the reference method can be attributed to multiple scattering from the same interface effect. Then it could be interesting to calculate this contribution in the model in order to quantify the contribution of each multiple scattering phenomenon. The contribution of double scattering in reflection from the same interface could rather easily be incorporated, as other papers present results for this specific contribution [23–25].

In addition, in the validity domain of the IKA+GOA, the numerical results confirmed that the scattering coefficient is independent of the RMS surface heights σ_{hA} and σ_{hB} (which can have different values). Moreover, the use of the (qualitative) Rayleigh roughness criterion is a good means to evaluate the validity of neglecting the coherent component of the scattering coefficient (which corresponds to the validity of using the GOA to quantify the scattering coefficient). By defining a Rayleigh parameter $Ra_{r,n}$ associated with each scattering coefficient $\sigma_{r,n}$ from the rough layer, it provided us an interesting means to evaluate the validity domain of the GOA of the IKA+GOA in a simple and fast way. It allowed us to observe that for one rough interface, the GOA can be applied for RMS surface height σ_{hA} down to approximately 0.25λ (for moderate incidence angles θ_i), which is in agreement with results from [32]. For two rough interfaces, the same condition applies, and when the first-order contribution can be neglected in comparison with the second-order one (like here where ϵ_{r2} is close to 1 and ϵ_{r3} is much greater than 1), it can be applied to even lower RMS surface heights. For instance, when $\sigma_{hA} = \sigma_{hB}$, it can be applied for moderate θ_i down to at least 0.20λ (and nearly 0.15λ). Thus, the IKA+GOA method provides an interesting means to calculate scattering from rough layers, which can be of moderate roughness σ_h.

APPENDIX A: CALCULATION OF THE SECOND-ORDER REFLECTION SCATTERING COEFFICIENT $\sigma_{r,2}$: COINCIDENTAL CONTRIBUTION

In this appendix, to facilitate notation, we choose to substitute the subscripts $-,1$ for $-$ and $+,1$ for $+$. Then the second-order reflected scattered field $E_{r,2}$ is written in the far field as [1]

$$E_{r,2} = \left(\frac{k_2}{2\pi}\right)^2 \left(\frac{k_1}{2\pi r}\right)^{1/2} E_0 e^{i(k_1 r - \pi/4)} \int \mathrm{d}\theta_- \mathrm{d}\theta_+ \mathrm{d}x_{A_1} \mathrm{d}x_{B_1} \mathrm{d}x_{A_2} \Xi(x_{A_1}) \Xi(x_{B_1}) \Xi(x_{A_2}) t_{12}(\chi_{ti}^0) g_{12}(\boldsymbol{k}_i, \boldsymbol{k}_-; \boldsymbol{n}_{ti}^0)$$
$$\times r_{23}(\chi_{r-}^0) f(\boldsymbol{k}_-, \boldsymbol{k}_+; \boldsymbol{n}_{r-}^0) t_{21}(\chi_{t+}^0) g_{21}(\boldsymbol{k}_+, \boldsymbol{k}_r; \boldsymbol{n}_{t+}^0) e^{i(\boldsymbol{k}_i \cdot \boldsymbol{r}_{A_1} - \boldsymbol{k}_r \cdot \boldsymbol{r}_{A_2})} e^{i(\boldsymbol{k}_- \cdot \boldsymbol{r}_{A_1 B_1} + \boldsymbol{k}_+ \cdot \boldsymbol{r}_{B_1 A_2})}, \quad \text{(A1)}$$

with $x_{A_1}, x_{B_1}, x_{A_2} \in [-L_0/2; +L_0/2]$, and $\theta_-, \theta_+ \in [-\pi/2; +\pi/2]$. The scattered field $E_{r,2}^*$ is obtained from taking the complex conjugate of Eq. (A1) and substituting the variables $\{\theta_-, \theta_+, \boldsymbol{k}_-, \boldsymbol{k}_+, x_{A_1}, x_{B_1}, x_{A_2}, z_{A_1}, z_{B_1}, z_{A_2}\}$ for $\{\theta'_-, \theta'_+, \boldsymbol{k}'_-, \boldsymbol{k}'_+, x_{A'_1}, x_{B'_1}, x_{A'_2}, z_{A'_1}, z_{B'_1}, z_{A'_2}\}$. Indeed, as the points of successive scattering are *a priori* different, the propagation directions and angles are different.

To calculate the power $p_{r,22} = \langle |E_{r,2}|^2 \rangle$, the GOA is used on both interfaces, at each point of scattering A_1, B_1, and A_2. It implies that only closely located correlated points contribute to the scattering power. Here two different cases can be considered: First, the coincident case, where the point A'_1 is close to A_1, B'_1 is close to B_1, and A'_2 is close to A_2. Second, the anticoincident case, where the point A'_1

is close to A_2, B_1' is close to B_1, and A_2' is close to A_1.The anticoincidental case contributes only around the antispecular (backscattering) direction. Here we focus on the coincidental case.

Both surfaces being stationary, the following variable transformations from $\{x_{A_1},x_{B_1},x_{A_2},x_{A_1'},x_{B_1'},x_{A_2'}\}$ into $\{x_{mA1},x_{mA2},x_{pA1},x_{pB1},x_{pA2}\}$ are used:

$$\left.\begin{aligned} x_{mA1} &= x_{A_1'} - x_{A_1} \\ x_{mB1} &= x_{B_1'} - x_{B_1} \\ x_{mA2} &= x_{A_2'} - x_{A_2} \\ x_{pA1} &= x_{A_1'} + x_{A_1} \\ x_{pB1} &= x_{B_1'} + x_{B_1} \\ x_{pA2} &= x_{A_2'} + x_{A_2} \end{aligned}\right\} \Rightarrow \left\{\begin{aligned} x_{A_1} &= (x_{pA1} - x_{mA1})/2 \\ x_{A_1'} &= (x_{pA1} + x_{mA1})/2 \\ x_{B_1} &= (x_{pB1} - x_{mB1})/2 \\ x_{B_1'} &= (x_{pB1} + x_{mB1})/2 \\ x_{A_2} &= (x_{pA2} - x_{mA2})/2 \\ x_{A_2'} &= (x_{pA2} + x_{mA2})/2 \end{aligned}\right. . \tag{A2}$$

The same variable transformations from $\{z_{A_1},z_{B_1},z_{A_2},z_{A_1'},z_{B_1'},z_{A_2'}\}$ into $\{z_{mA1},z_{mA2},z_{pA1},z_{pB1},z_{pA2}\}$ are used.

The GOA is used on both interfaces. Then only closely located correlated points of the surface contribute to the scattering coefficient, and the following approximations can be made: $z_{mA1}=z_{A_1'}-z_{A_1}\approx\gamma_{A_1}(x_{A_1'}-x_{A_1})=\gamma_{A_1}x_{mA1}$, $z_{mB1}\approx\gamma_{B_1}x_{mB1}$, $z_{mA2}\approx\gamma_{A_2}x_{mA2}$, $x_{pA1}=x_{A_1'}+x_{A_1}\approx 2x_{A_1}$, $z_{pA1}=z_{A_1'}+z_{A_1}\approx 2z_{A_1}$, $x_{pB1}\approx 2x_{B_1}$, $z_{pB1}\approx 2z_{B_1}$, $x_{pA2}\approx x_{A_2}$, and $z_{pA2}\approx z_{A_2}$. This way, the real variable transformations made are $\{x_{A_1},x_{B_1},x_{A_2},x_{A_1'},x_{B_1'},x_{A_2'}\}$ into $\{x_{A_1},x_{B_1},x_{A_2},x_{mA1},x_{mA2}\}$. Then the expression of the statistical correlation of $E_{r,2}$ is given by

$$\begin{aligned}\langle|E_{r,2}|^2\rangle = \left(\frac{k_2}{2\pi}\right)^4 \frac{k_1}{2\pi r}|E_0|^2 \int & dx_{A_1}dx_{B_1}dx_{A_2}dx_{mA1}dx_{mB1}dx_{mA2}d\theta_-d\theta_-'d\theta_+d\theta_+'t_{12}(\chi_{ti}^0)t_{12}^*(\chi_{ti}'^0)g_{12}(\hat{\boldsymbol{k}}_i,\hat{\boldsymbol{k}}_-;\boldsymbol{n}_{ti}^0)g_{12}(\hat{\boldsymbol{k}}_i,\\ &\times\hat{\boldsymbol{k}}_-';\boldsymbol{n}_{ti}^0)r_{23}(\chi_{r-}^0)r_{23}^*(\chi_{r-}'^0)f(\hat{\boldsymbol{k}}_-,\hat{\boldsymbol{k}}_+;\boldsymbol{n}_{r-}^0)f(\hat{\boldsymbol{k}}_-',\hat{\boldsymbol{k}}_+';\boldsymbol{n}_{r-}^0)t_{21}(\chi_{t+}^0)t_{21}^*(\chi_{t+}'^0)g_{21}(\hat{\boldsymbol{k}}_+,\hat{\boldsymbol{k}}_r;\boldsymbol{n}_{t+}^0)g_{21}(\hat{\boldsymbol{k}}_+',\hat{\boldsymbol{k}}_r;\boldsymbol{n}_{t+}^0)\\ &\times e^{i[-(k_2\hat{k}_- - k_2^*\hat{k}_-')x_{A_1}+(k_2\hat{k}_- - k_2^*\hat{k}_-' - k_2\hat{k}_+ + k_2^*\hat{k}_+')x_{B_1}+(k_2\hat{k}_+ - k_2^*\hat{k}_+')x_{A_2}]}\langle\Xi(x_{A1})\Xi(x_{B1})\Xi(x_{A2})\Xi(x_{A'1})\Xi(x_{B'1})\Xi(x_{A'2})\\ &\times e^{i\{-k_1(k_i+\gamma_{tA_1}\hat{q}_i)+[(k_2\hat{k}_- - k_2^*\hat{k}_-')+\gamma_{tA_1}(k_2\hat{q}_- + k_2^*\hat{q}_-')]/2\}x_{mA1}}e^{-i/2[(k_2\hat{k}_- + k_2^*\hat{k}_-' - k_2\hat{k}_+ - k_2^*\hat{k}_+')+\gamma_{rB_1}(k_2\hat{q}_- + k_2^*\hat{q}_-' - k_2\hat{q}_+ - k_2^*\hat{q}_+')]x_{mB1}}\\ &\times e^{i\{k_1(k_r+\gamma_{tA_2}\hat{q}_r)-[(k_2\hat{k}_+ + k_2^*\hat{k}_+')+\gamma_{tA_2}(k_2\hat{q}_+ + k_2^*\hat{q}_+')]/2\}x_{mA2}}e^{i[-(k_2\hat{q}_- - k_2^*\hat{q}_-')z_{A_1}+(k_2\hat{q}_- - k_2^*\hat{q}_- - k_2\hat{q}_+ + k_2^*\hat{q}_+')z_{B_1}+(k_2\hat{q}_+ - k_2^*\hat{q}_+')z_{A_2}]}\rangle,\end{aligned} \tag{A3}$$

with $\{x_{mA1},x_{mB1},x_{mA2}\}\in[-L_0;+L_0]$. In the latter equation, the random variables are $\{z_{A_1},z_{B_1},z_{A_2},\gamma_{A_1},\gamma_{B_1},\gamma_{A_2},\Xi\}$, with $\Xi=[\Xi(x_{A1})\Xi(x_{B1})\Xi(x_{A2})\Xi(x_{A'1})\Xi(x_{B'1})\Xi(x_{A'2})]$. The PDF $p(z_{A_1},z_{B_1},z_{A_2},\gamma_{A_1},\gamma_{B_1},\gamma_{A_2},\Xi)$ is expressed in terms of the conditional density $p(\Xi|z_{A_1},z_{B_1},z_{A_2},\gamma_{A_1},\gamma_{B_1},\gamma_{A_2})$ as

$$p(z_{A_1},z_{B_1},z_{A_2},\gamma_{A_1},\gamma_{B_1},\gamma_{A_2},\Xi) = p(z_{A_1},z_{B_1},z_{A_2},\gamma_{A_1},\gamma_{B_1},\gamma_{A_2}) \times p(\Xi|z_{A_1},z_{B_1},z_{A_2},\gamma_{A_1},\gamma_{B_1},\gamma_{A_2}), \tag{A4}$$

where the last term in Eq. (A4) is expressed by

$$\begin{aligned} p(\Xi|z_{A_1},z_{B_1},z_{A_2},\gamma_{A_1},\gamma_{B_1},\gamma_{A_2}) = {} & S_{1221}(\theta_i,\theta_-,\theta_+,\theta_r|z_{A_1},z_{B_1},z_{A_2},\gamma_{A_1},\gamma_{B_1},\gamma_{A_2})\,\delta(\Xi-\boldsymbol{1})\\ & + [1 - S_{1221}(\theta_i,\theta_-,\theta_+,\theta_r|z_{A_1},z_{B_1},z_{A_2},\gamma_{A_1},\gamma_{B_1},\gamma_{A_2})]\delta(\Xi), \end{aligned} \tag{A5}$$

with Ξ, $\boldsymbol{1}=[1\ 1\ 1\ 1\ 1\ 1]$ are vectors of length six; $p(z_{A_1},z_{B_1},z_{A_2},\gamma_{A_1},\gamma_{B_1},\gamma_{A_2})$ stands for the surface height and slope joint distribution, whose covariance matrix is expressed as follows:

$$[C_6] = \begin{bmatrix} \sigma_{hA}^2 & \rho_{A_1B_1} & \rho_{A_1A_2} & 0 & \rho'_{A_1B_1} & \rho'_{A_1A_2} \\ \rho_{A_1B_1} & \sigma_{hB}^2 & \rho_{B_1A_2} & -\rho'_{A_1B_1} & 0 & \rho'_{B_1A_2} \\ \rho_{A_1A_2} & \rho_{B_1A_2} & \sigma_{hA}^2 & -\rho'_{A_1A_2} & -\rho'_{B_1A_2} & 0 \\ 0 & -\rho'_{A_1B_1} & -\rho'_{A_1A_2} & \sigma_{sA}^2 & \rho''_{A_1B_1} & \rho''_{A_1A_2} \\ \rho'_{A_1B_1} & 0 & -\rho'_{B_1A_2} & \rho''_{A_1B_1} & \sigma_{sB}^2 & \rho''_{B_1A_2} \\ \rho'_{A_1A_2} & \rho'_{B_1A_2} & 0 & \rho'_{A_1A_2} & \rho''_{B_1A_2} & \sigma_{sA}^2 \end{bmatrix}. \tag{A6}$$

It must be noted that the height correlations ρ are even, where $\rho_{A_1A_2}=\rho(x_{A_1A_2})=\rho(x_{A_2}-x_{A_1})$ is the height autocorrelation of Σ_A, and $\rho_{A_1B_1}$, $\rho_{B_1A_2}$ are height cross correlations between Σ_A and Σ_B. As ρ is even, ρ' is odd, and ρ'' is even.

In addition, $\rho(0)=\sigma_h^2$, $\rho'(0)=0$, and $\rho''(0)=-\sigma_s^2$ (σ_s is the RMS slope of the surface considered). For a stationary process, one can note that the covariance matrix is independent of $\{x_{mA1},x_{mB1},x_{mA2}\}$.

Then the statistical averaging in Eq. (A3) over the illumination functions yields

$$\langle \Xi \rangle = S_{1221}(\theta_i, \theta_-, \theta_+, \theta_r | z_{A_1}, z_{B_1}, z_{A_2}, \gamma_{A_1}, \gamma_{B_1}, \gamma_{A_2}). \quad \text{(A7)}$$

Here the two surfaces are assumed to be uncorrelated, and so are A_1 and A_2 ($x_{A_1A_2} \gg L_{cA}$). Thus, as a general rule in this method (for the coincidental case), all the points of successive reflections are assumed to be uncorrelated between one another. Then the only term in Eq. (A3) that depends on x_{A_1} is the term inside the corresponding exponential. As we assumed that the upper surface length $L_0 \gg L_{cA}$, the integration over x_{A_1} reduces to

$$\int_{-L_0/2}^{+L_0/2} \exp[i(k_2 \hat{k}'_- - k_2^* \hat{k}_-) x_{A_1}] \mathrm{d}x_{A_1} = \frac{2\pi}{|k_2|} \delta\left(\frac{k_2^*}{k_2} \hat{k}'_- - \hat{k}_- \right); \quad \text{(A8)}$$

therefore, as $\hat{k}'_-$ and $\hat{k}_-$ are both real, $k_2^* = k_2$ (which means that the inner medium Ω_2 is lossless, that is to say, $\epsilon_{r2} \in \mathbb{R}$) and $\hat{k}'_- = \hat{k}_-$, $\theta'_- = \theta_-$, and $\hat{q}'_- = \hat{q}_-$. Then the integration over θ'_- can be suppressed. Using the same method for x_{A_2}, we obtain

$$\int_{-L_0/2}^{+L_0/2} \exp[ik_2(\hat{k}_+ - \hat{k}'_+) x_{A_2}] \mathrm{d}x_{A_2} = \frac{2\pi}{|k_2|} \delta(\hat{k}_+ - \hat{k}'_+), \quad \text{(A9)}$$

which implies that $\hat{k}'_+ = \hat{k}_+$, $\theta'_+ = \theta_+$, and $\hat{q}'_+ = \hat{q}_+$. We also have $\chi'^0_{ti} = \chi^0_{ti}$, $\chi'^0_{t-} = \chi^0_{t-}$, $\chi'^0_{r-} = \chi^0_{r-}$, and $\chi'^0_{t+} = \chi^0_{t+}$. Then the integration over θ'_+ can be suppressed. Using the same method for x_{B_1}, we obtain

$$\int_{-L_0/2}^{+L_0/2} \exp[ik_2(\hat{k}_- - \hat{k}'_- - \hat{k}_+ + \hat{k}'_+) x_{B_1}] \mathrm{d}x_{B_1} = L_0. \quad \text{(A10)}$$

Then one can notice that the term inside the exponential, which depends on the heights, equals zero. Thus, the statistical averaging over the heights and slopes, $p(z_{A_1}, z_{B_1}, z_{A_2}, \gamma_{A_1}, \gamma_{B_1}, \gamma_{A_2})$, reduces to the slopes only, $p_s(\gamma^0_{A_1}, \gamma^0_{B_1}, \gamma^0_{A_2})$. Moreover, as the points A_1, B_1, and A_2 are uncorrelated between one another, this reduces to $p_s(\gamma^0_{tA_1}) p_s(\gamma^0_{rB_1}) p_s(\gamma^0_{tA_2})$, and

$$S_{1221}(\theta_i, \theta_-, \theta_+, \theta_r | z_{A_1}, z_{B_1}, z_{A_2}, \gamma_{A_1}, \gamma_{B_1}, \gamma_{A_2}) = S_{12}(\theta_i, \theta_- | \gamma^0_{tA_1}) S_{22}(\theta_-, \theta_+ | \gamma^0_{tB_1}) S_{21}(\theta_+, \theta_r | \gamma^0_{tA_2}),$$

where each term is averaged over the heights.

In Eq. (A3), the only term that depends on x_{mA1} is the term inside the corresponding exponential. Assuming that $L_0 \gg L_{cA}$, the integration over x_{mA1} leads to

$$\int_{-L_0}^{+L_0} \exp\{i[(-k_1 \hat{k}_i + k_2 \hat{k}_-) + \gamma_{tA_1}(-k_1 \hat{q}_i + k_2 \hat{q}_-)] x_{mA1}\} \mathrm{d}x_{mA1} = \frac{2\pi}{|k_2||\hat{q}_- - (k_1/k_2)\hat{q}_i|} \delta\left(\gamma_{tA_1} + \frac{k_2 \hat{k}_- - k_1 \hat{k}_i}{k_2 \hat{q}_- - k_1 \hat{q}_i} \right). \quad \text{(A11)}$$

Using the same method for x_{mB1}, assuming that L_0 is much greater than the lower surface correlation length L_{cB}, one obtains

$$\int_{-L_0}^{+L_0} \exp\{-ik_2[(\hat{k}_- - \hat{k}_+) + \gamma_{rB_1}(\hat{q}_- - \hat{q}_+)] x_{mB1}\} \mathrm{d}x_{mB1} = \frac{2\pi}{|k_2||\hat{q}_+ - \hat{q}_-|} \delta\left(\gamma_{rB_1} + \frac{\hat{k}_+ - \hat{k}_-}{\hat{q}_+ - \hat{q}_-} \right). \quad \text{(A12)}$$

Using the same method for x_{mA2}, as we assumed $L_0 \gg L_{cA}$, one obtains

$$\int_{-L_0}^{+L_0} \exp\{i[(k_1 \hat{k}_r - k_2 \hat{k}_+) + \gamma_{tA_2}(k_1 \hat{q}_r - k_2 \hat{q}_+)] x_{mA2}\} \mathrm{d}x_{mA2} = \frac{2\pi}{|k_1||\hat{q}_r - (k_2/k_1)\hat{q}_+|} \delta\left(\gamma_{tA_2} + \frac{k_1 \hat{k}_r - k_2 \hat{k}_+}{k_1 \hat{q}_r - k_2 \hat{q}_+} \right). \quad \text{(A13)}$$

Thus, one obtains the expressions of the slopes given by Eqs. (3)–(5).

The calculus of $p_{r,12} = 2\,\Re e(\langle E_{r,1} E^*_{r,2} \rangle)$ uses the same approximations and is consequently not presented here. The approximations used imply in the calculus of $p_{r,12}$ that $\hat{q}_- = 0$, that is to say, $\theta_- = \pm \pi/2$, which implies that $p_{r,12} = 0$ owing to the shadow. Let us note that this means there is no correlation between $E_{r,1}$ and $E_{r,2}$. Eventually, using the general relation for the scattering coefficient $\sigma_r = r p_r / (|E_i|^2 L_0 \cos\theta_i)$, with $p_{r,2} = p_{r,22}$, we obtain the expression of Eq. (2).

APPENDIX B: CALCULATION OF THE COHERENT CONTRIBUTION $\sigma^{coh}_{r,1}$

From the expression of the first-order reflection scattered field $E_{r,1}$ [see Eq. 5 of [1]], the coherent reflection scattering coefficient $\sigma^{coh}_{r,1}$ can be expressed as follows:

$$\sigma^{coh}_{r,1}(\boldsymbol{k}_r, \boldsymbol{k}_i) = \frac{1}{\cos\theta_i} \frac{k_1}{2\pi L_A} |r_{12}(\chi^0_{ri}) f(\boldsymbol{k}_i, \boldsymbol{k}_r; \boldsymbol{n}^0_{ri})|^2 \times |\langle e^{i(q_i - q_r)\zeta_A} S_{11}(\boldsymbol{k}_i, \boldsymbol{k}_r | \zeta_A) \rangle|^2 \times L_A^2 \,\mathrm{sinc}^2\left[(\hat{k}_r - \hat{k}_i) \frac{L_A}{2} \right], \quad \text{(B1)}$$

with $\mathrm{sinc}(x) = \sin(x)/x$. Under the assumption that the upper surface length L_A is large compared to the incident wavelength λ, $L_A \gg \lambda$, $\sigma^{coh}_{r,1}$ becomes

$$\sigma^{coh}_{r,1}(\boldsymbol{k}_r, \boldsymbol{k}_i) \simeq \frac{1}{\cos\theta_i} \frac{k_1}{2\pi L_A} |r_{12}(\chi^0_{ri}) f(\boldsymbol{k}_i, \boldsymbol{k}_r; \boldsymbol{n}^0_{ri})|^2 \times \left| \langle e^{i(q_i - q_r)\zeta_A} S_{11}(\boldsymbol{k}_i, \boldsymbol{k}_r | \zeta_A) \rangle \right|^2 \left(\frac{k_1}{2\pi L_A} \right)^2 \times \delta^2(\hat{k}_r - \hat{k}_i) \quad \text{(B2)}$$

By assuming that the shadowing function S_{11} and the term $\exp[i(q_i - q_r)\zeta_A]$ are uncorrelated, the statistical average over the heights ζ_A becomes

$$\langle e^{i(q_i - q_r)\zeta_A} S_{11}(\boldsymbol{k}_i, \boldsymbol{k}_r | \zeta_A) \rangle = \langle e^{i(q_i - q_r)\zeta_A} \rangle S_{11}(\boldsymbol{k}_i, \boldsymbol{k}_r), \quad \text{(B3)}$$

where $S_{11}(\boldsymbol{k}_i \boldsymbol{k}_r)$ is the shadowing function averaged over the surface heights.

The statistical average $\langle \exp[i(q_i-q_r)\zeta_A]\rangle$ is equal to the characteristic function $\chi_h(q_i-q_r)$ such that

$$\chi_h(q_i-q_r) \equiv \langle e^{i(q_i-q_r)\zeta_A}\rangle = \int_{-\infty}^{+\infty} e^{i(q_i-q_r)\zeta_A} p_h(\zeta_A)\mathrm{d}\zeta_A. \quad \text{(B4)}$$

The result depends then on the surface statistics: The height PDF $p_h(\zeta_A)$ is in general equal to a Gaussian with zero-mean value

$$p_h(\zeta_A) = \frac{1}{\sigma_h\sqrt{2\pi}}\exp\left[-\left(\frac{\zeta_A}{\sqrt{2}\sigma_h}\right)^2\right]. \quad \text{(B5)}$$

Then the characteristic function is given by

$$\chi_h(q_i-q_r) \equiv \langle e^{i(q_i-q_r)\zeta_A}\rangle = e^{-2Ra_{r12}^{A\,2}}, \quad \text{(B6)}$$

with

$$Ra_{r12}^{A} = \frac{|q_i-q_r|}{2}\sigma_{hA} \quad \text{(B7)}$$

being the general Rayleigh roughness parameter expressed for the case of reflection from the upper interface Σ_A.

Thus, the coherent reflection scattering coefficient is given by

$$\sigma_{r,1}^{coh}(\boldsymbol{k}_r,\boldsymbol{k}_i) = \frac{1}{\cos\theta_i}\frac{2\pi}{k_1 L_A}|r_{12}(\chi_{ri}^0) f(\boldsymbol{k}_i,\boldsymbol{k}_r;\boldsymbol{n}_{ri}^0)|^2 \times \mathcal{A}_{r,1} S_{11}^2(\boldsymbol{k}_i,\boldsymbol{k}_r)\delta(\hat{k}_r-\hat{k}_i), \quad \text{(B8)}$$

with $\mathcal{A}_{r,1}=|\chi_h(q_i-q_r)|^2$ the power loss parameter, expressed for Gaussian statistics by

$$\mathcal{A}_{r,1} = e^{-g_{r,1}}, \quad \text{where} \quad g_{r,1} = 4Ra_{r12}^{A\,2} = |q_i-q_r|^2\sigma_{hA}^2. \quad \text{(B9)}$$

The Dirac delta function accounts for the fact that for a surface length L_A much greater than the wavelength λ, the coherent power scattered by the rough surface occurs only in the specular direction.

For a surface of Lorentzian or exponential height PDF, the coherent power loss due to the roughness takes a different form. For instance, for exponential statistics with zero average,

$$p_h(\zeta_A) = \frac{1}{\sqrt{2}\sigma_{hA}}\exp\left[-\frac{\sqrt{2}|\zeta_A|}{\sigma_{hA}}\right], \quad \text{(B10)}$$

the power loss parameter is given by

$$\mathcal{A}_{r,1} = \frac{1}{(1+Ra_{r12}^{A})^2} = \frac{1}{(1+g_{r,1}/2)^2}. \quad \text{(B11)}$$

APPENDIX C: CALCULATION OF $\sigma_{t,1}^{coh}$ AND $\sigma_{r,2}^{coh}$

Using the same method as for $\sigma_{r,1}^{coh}$, the coherent scattering coefficients $\sigma_{t,1}^{coh}$ and $\sigma_{r,2}^{coh}$ can easily be obtained from the expressions of the corresponding scattered fields, namely, $E_{t,1}$ given by Eq. (8) of [1], and $E_{r,2}$ given by Eq. (A1), respectively.

Then, under the hypothesis that the length L_0 of both surfaces, $L_0=L_A=L_B$, is much greater than the wavelength λ, the coherent contributions occur only in the specular direction, and they are expressed for uncorrelated shadowing functions by

$$\sigma_{t,1}^{coh}(\boldsymbol{k}_t^{sp},\boldsymbol{k}_i) = \frac{\eta_1}{\eta_3}\frac{1}{\cos\theta_i}\frac{2\pi}{k_3 L_A} \times |t_{12}(\theta_i) g_{12}(\boldsymbol{k}_i,\boldsymbol{k}_{-,1}^{sp};\boldsymbol{z}) t_{23}(\theta_{-,1}) g_{23}(\boldsymbol{k}_{-,1}^{sp},\boldsymbol{k}_t^{sp};\boldsymbol{z})|^2 \times \mathcal{A}_{t,1} S_{12}^2(\boldsymbol{k}_i,\boldsymbol{k}_{-,1}^{sp}) S_{23}^2(\boldsymbol{k}_{-,1}^{sp},\boldsymbol{k}_t^{sp}), \quad \text{(C1)}$$

$$\sigma_{r,2}^{coh}(\boldsymbol{k}_r^{sp},\boldsymbol{k}_i) = \frac{1}{\cos\theta_i}\frac{2\pi}{k_1 L_A}|t_{12}(\theta_i) g_{12}(\boldsymbol{k}_i,\boldsymbol{k}_{-,1}^{sp};\boldsymbol{z})|^2 \times |r_{23}(\theta_{-,1}) f(\boldsymbol{k}_{-,1}^{sp},\boldsymbol{k}_{+,1}^{sp};\boldsymbol{z}) t_{21}(\theta_{+,1}) g_{21}(\boldsymbol{k}_{+,1}^{sp},\boldsymbol{k}_r^{sp};\boldsymbol{z})|^2 \times \mathcal{A}_{r,2} S_{12}^2(\boldsymbol{k}_i,\boldsymbol{k}_{-,1}^{sp}) S_{22}^2(\boldsymbol{k}_{-,1}^{sp},\boldsymbol{k}_{+,1}^{sp}) S_{21}^2(\boldsymbol{k}_{+,1}^{sp},\boldsymbol{k}_t^{sp}), \quad \text{(C2)}$$

where $\mathcal{A}_{t,1}=|\chi_h(q_i-q_{-,1}^{sp})\chi_h(q_{-,1}^{sp}-q_t^{sp})|^2$, and $\mathcal{A}_{r,2}=|\chi_h(q_i-q_{-,1}^{sp})\chi_h(q_{-,1}^{sp}-q_{+,1}^{sp})\chi_h(q_{+,1}^{sp}-q_r^{sp})|^2$. The local normal to the considered surface $\mathbf{n}^0$ is equal to the vertical direction $\mathbf{z}$. The specular terms, denoted in superscript as *sp*, are given by the Snell–Descartes laws $\sqrt{\epsilon_{r2}}\sin\theta_{-,1}^{sp}=\sqrt{\epsilon_{r1}}\sin\theta_i$, $\sqrt{\epsilon_{r3}}\sin\theta_t^{sp}=\sqrt{\epsilon_{r2}}\sin\theta_{-,1}^{sp}$, $\theta_{+,1}^{sp}=-\theta_{-,1}^{sp}$, and $\sqrt{\epsilon_{r1}}\sin\theta_r^{sp}=\sqrt{\epsilon_{r2}}\sin\theta_{+,1}^{sp}$ (with $\epsilon_{r\alpha}$ the relative permittivity of medium Ω_α). For a Gaussian height PDF, the general term $\chi_h(q_\alpha-q_\beta)$ is given by

$$\chi_h(q_\alpha-q_\beta) = e^{-g_{s\alpha\beta}/2}, \quad \text{where} \quad g_{s\alpha\beta} = 4Ra_{s\alpha\beta}^{M\,2} = |q_\alpha-q_\beta|^2\sigma_{hM}^2, \quad \text{(C3)}$$

with $M\equiv A$ at the upper interface Σ_A and $M\equiv B$ at the upper interface Σ_B, and the subscript β corresponding to the medium Ω_β of the scattered wave, for which $s\equiv r$ for the

case of scattering in reflection and $s \equiv t$ for the case of scattering in transmission.

By comparison, for $L_0 \gg \lambda$, $\sigma_{r,1}^{coh}$, which in consequence also occurs only in the specular direction, is expressed by

$$\sigma_{r,1}^{coh}(\boldsymbol{k}_r^{sp}, \boldsymbol{k}_i) = \frac{1}{\cos\theta_i} \frac{2\pi}{k_1 L_A} |r_{12}(\theta_i) f(\boldsymbol{k}_i, \boldsymbol{k}_r^{sp}; \boldsymbol{z})|^2 \times \mathcal{A}_{r,1} S_{11}^2(\boldsymbol{k}_i, \boldsymbol{k}_r^{sp}). \quad \text{(C4)}$$

The specular terms, denoted in superscript as sp, are given by the Snell–Descartes law $\theta_r^{sp} = -\theta_i$.

ACKNOWLEDGMENTS

The authors would like to thank the reviewers for their useful and constructive comments.

REFERENCES

1. N. Pinel, N. Déchamps, C. Bourlier, and J. Saillard, "Bistatic scattering from one-dimensional random rough homogeneous layers in the high-frequency limit with shadowing effect," Waves Random Complex Media **17**, 283–303 (2007).
2. P. Beckmann and A. Spizzichino, *The Scattering of Electromagnetic Waves from Rough Surfaces* (Pergamon, 1963).
3. J. Ogilvy, *Theory of Wave Scattering from Random Surfaces* (Institute of Physics, 1991).
4. J. A. Kong, *Electromagnetic Wave Theory*, 2nd ed. (Wiley, 1990).
5. A. Fung, *Microwave Scattering and Emission Models and Their Applications* (Artech, 1994).
6. J. Caron, J. Lafait, and C. Andraud, "Scalar Kirchhoff's model for light scattering from dielectric random rough surfaces," Opt. Commun. **207**, 17–28 (2002).
7. C. Bourlier, G. Berginc, and J. Saillard, "Monostatic and bistatic statistical shadowing functions from a one-dimensional stationary randomly rough surface according to the observation length: I. Single scattering," Waves Random Media **12**, 145–173 (2002).
8. N. Pinel, C. Bourlier, and J. Saillard, "Energy conservation of the scattering from rough surfaces in the high-frequency limit," Opt. Lett. **30**, 2007–2009 (2005).
9. N. Pinel, C. Bourlier, and J. Saillard, "Forward radar propagation over oil slicks on sea surfaces using the Ament model with shadowing effect," Prog. Electromagn. Res. **76**, 95–126 (2007).
10. N. Déchamps, N. de Beaucoudrey, C. Bourlier, and S. Toutain, "Fast numerical method for electromagnetic scattering by rough layered interfaces: propagation-inside-layer expansion method," J. Opt. Soc. Am. A **23**, 359–369 (2006).
11. N. Déchamps and C. Bourlier, "Electromagnetic scattering from a rough layer: propagation-inside-layer expansion method combined to the forward-backward novel spectral acceleration," IEEE Trans. Antennas Propag. **55**, 3576–3586 (2007).
12. A. Iodice, "Forward-backward method for scattering from dielectric rough surfaces," IEEE Trans. Antennas Propag. **50**, 901–911 (2002).
13. H.-T. Chou and J. Johnson, "A novel acceleration algorithm for the computation of scattering from rough surfaces with the forward-backward method," Radio Sci. **33**, 1277–1287 (1998).
14. H.-T. Chou and J. Johnson, "Formulation of forward-backward method using novel spectral acceleration for the modeling of scattering from impedance rough surfaces," IEEE Trans. Geosci. Remote Sens. **38**, 605–607 (2000).
15. D. Torrungrueng and J. Johnson, "Some issues related to the novel spectral acceleration method for the fast computation of radiation/scattering from one-dimensional extremely large scale quasi-planar structures," Radio Sci. **37**, 1019 (2002).
16. C. Moss, T. Grzegorczyk, H. Han, and J. Kong, "Forward-backward method with spectral acceleration for scattering from layered rough surfaces," IEEE Trans. Antennas Propag. **54**, 2917–2929 (2006).
17. N. Pinel, "Etude de modèles asymptotiques de la diffusion des ondes électromagnétiques par des interfaces naturelles — application à une mer recouverte de pétrole," Ph.D. thesis (Ecole Polytechnique de l'Université de Nantes, 2006).
18. P. Lynch, "Curvature corrections to rough-surface scattering at high frequencies," J. Acoust. Soc. Am. **47**, 804–815 (1970).
19. F. Bass and I. Fuks, *Wave Scattering from Statistically Rough Surfaces* (Pergamon, 1978).
20. A. Voronovich, *Wave Scattering from Rough Surfaces*, 2nd ed. (Springer, 1999).
21. R. Papa and J. Lennon, "Conditions for the validity of physical optics in rough surface scattering," IEEE Trans. Antennas Propag. **36**, 647–650 (1988).
22. A. Collaro, G. Franceschetti, M. Migliaccio, and D. Riccio, "Gaussian rough surfaces and Kirchhoff approximation," IEEE Trans. Antennas Propag. **47**, 392–398 (1999).
23. E. Bahar and M. El-Shenawee, "Double-scatter cross sections for two-dimensional random rough surfaces that exhibit backscatter enhancement," J. Opt. Soc. Am. A **18**, 108–116 (2001).
24. A. Ishimaru, C. Le, Y. Kuga, L. Sengers, and T. Chan, "Polarimetric scattering theory for high slope rough surfaces," Prog. Electromagn. Res. **14**, 1–36 (1996).
25. C. Bourlier and G. Berginc, "Multiple scattering in the high-frequency limit with second-order shadowing function from 2D anisotropic rough dielectric surfaces: I. Theoretical study," Waves Random Media **14**, 229–252 (2004).
26. P. Lynch and R. Wagner, "Rough-surface scattering: shadowing, multiple scatter, and energy conservation," J. Math. Phys. **11**, 3032–3042 (1970).
27. L. Tsang and J. Kong, "Energy conservation for reflectivity and transmissivity at a very rough surface," J. Appl. Phys. **51**, 673–680 (1980).
28. A. Fung and H. Eom, "Multiple scattering and depolarization by a randomly rough Kirchhoff surface," IEEE Trans. Antennas Propag. **AP-29**, 463–471 (1981).
29. H. Eom, "Energy conservation and reciprocity of random rough surface scattering," Appl. Opt. **24**, 1730–1732 (1985).
30. L. Tsang, J. Kong, K. Ding, and C. Ao, *Scattering of Electromagnetic Waves, Volume I: Theories and Applications* (Wiley, 2000).
31. N. Pinel, C. Bourlier, and J. Saillard, "Rayleigh parameter of a rough layer: application to forward radar propagation over oil slicks on sea surfaces under the Ament model," Microwave Opt. Technol. Lett. **49**, 2285–2290 (2007).
32. E. Thorsos, "The validity of the Kirchhoff approximation for rough surface scattering using a Gaussian roughness spectrum," J. Acoust. Soc. Am. **83**, 78–92 (1988).
33. P. Croce and L. Prod'homme, "On the conditions for applying light scattering methods to rough surface evaluation," J. Opt. **15**, 95–104 (1984).
34. J. Lu, A. Maradudin, and T. Michel, "Enhanced backscattering from a rough dielectric film on a reflecting substrate," J. Opt. Soc. Am. B **8**, 311–318 (1991).
35. N. Bruce, "On the validity of the inclusion of geometrical shadowing functions in the multiple-scatter Kirchhoff approximation," Waves Random Media **14**, 1–12 (2004).